UiT Norges arktiske universitet

Faculty of Science and Technology
Department of Geosciences

The Use of Foraminiferal Geochemistry to Investigate Methane Seepage at the Svyatogor Ridge, Arctic Ocean.

Abidemi Alex Akinselure
Master's Thesis in Geology [GEO-3900] May 2022

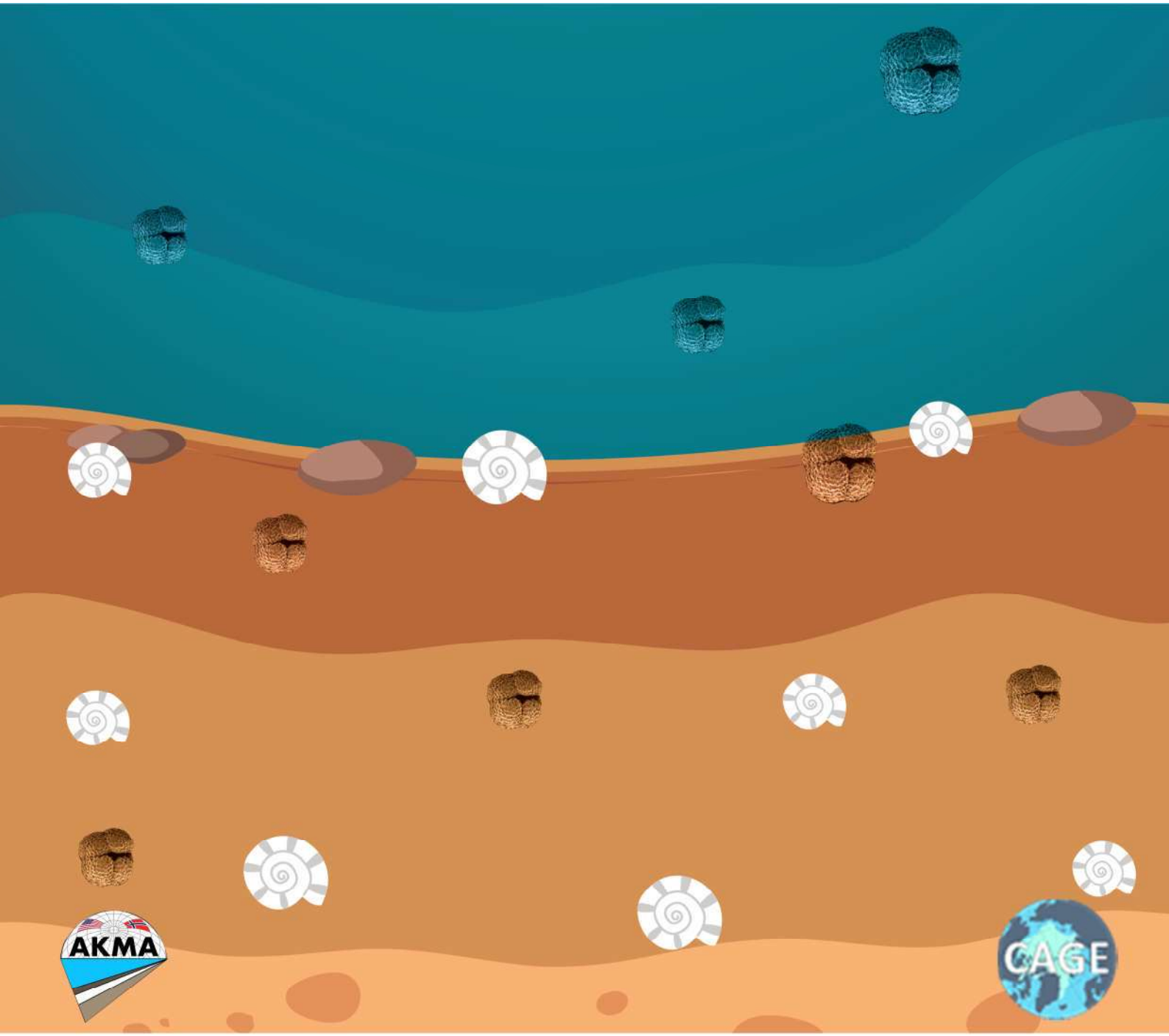

Abstract

Methane is a greenhouse gas contributing to contemporaneous global warming, and seepage is one of the ways through which it migrates from the deep sedimentary basins, all the way up to the hydro- and atmosphere. The study of methane seepage is still young as scientists are yet to discover most seep sites as well as seep associated biological species. A record of past methane seepage can be derived from the $\delta\ ^{13}C$ stored in the foraminiferal tests and in the seafloor sediments via precipitation of carbonate minerals by microbial oxidation of methane. In this study, the stable isotopes of carbon and oxygen of the foraminiferal tests were used alongside sediment geochemistry and organic compounds of the sediment as proxies to investigate methane seepage at the Svyatogor Ridge, Arctic Ocean. Two lithological units were recognised from the gravity core (GC3), corresponding to different sedimentation patterns during the last deglaciation. 158 - 162 cm and 137 – 142 cm intervals of the gravity core were impacted by anaerobic oxidation of methane (AOM) processes based on the Ba/Ti peaks which represent barite fronts immediately above sulfate-methane transition zones (SMTZs). Also, the vertical shift in between the paleo-SMTZs shows an upward fluid flow. The paleo-SMTZs in the gravity core (GC3) formed later than 14.5 ca ka BP. The organic matter in the blade core (BlaC3) is highly depleted due to bacterial mat biomass which incorporated methane-derived carbon. The stable carbon and oxygen isotopes of the tests show that the foraminifera calcified under normal marine conditions and during the Younger Dryas post-Bølling period. The C/N (Carbon/Nitrogen) elemental ratios show a predominantly marine origin for the sedimentary organic matter with some mix of land-derived and marine-derived organic matter. The organic carbon concentration (%C) shows that the sediments are of low productivity. An interval rich in ice-rafted debris with bivalve shells associated with high C/N values was found at 120 to 140 cm interval in the gravity core, suggesting sedimentary inputs from nearby Svalbard margin. A foraminiferal $\delta\ ^{13}C$ of -12.73 ‰ ~10 cm below this level indicates some secondary MDAC (Methane-derived authigenic carbonate) formation. It remains unclear whether the bivalves represent an ancient seep habitat or have been transported by icebergs from nearby Svalbard margin.

Acknowledgements

This research was supported by CAGE (Centre for Arctic Gas Hydrates, Environment and Climate) and AKMA (Advancing Knowledge on Methane in the Arctic).

First and foremost, I would like to express my heartfelt thanks to my main supervisor, Professor Giuliana Panieri, for the privilege to write my master's thesis under her supervision, as well as for her expertise and guidance during this project. Also, thanks to Dr. Claudio Argentino, my co-supervisor, for his attention and patience throughout this process.

I am extremely grateful to the laboratory personnel, Trine Dahl, Ingvild Hald, Karina Monsen, and Johan Matteus Lindgren, who made me feel very comfortable and were always available to answer my questions.

Finally, a big thank you to my friends and family for their encouragement and moral support throughout my studies. Most importantly, I would like to express my gratitude to God for making my coming to Norway a reality.

Abidemi Alex Akinselure

May 2022

CHAPTER 1

1. Introduction

1.1 Methane (CH_4) and Methane Seepage.

Methane is a greenhouse gas that contributes to global warming. Carbon and Hydrogen, in a 1:4 ratio, make up its fundamental elements. It is the dominant part of natural gas. Methane seeps occur when methane-rich fluids escape the seafloor. Methane seeps are areas in the marine environment where methane percolates through the sediments from below, occasionally releasing into the water column above (Schneider et al., 2018). Methane seepage occurs at temperatures similar to those in surrounding sediments, hence they are also called cold seeps (Levin, 2007). Methane emissions are associated with gas-oil seeps, mud volcanoes, micro seepage and submarine seepage in sedimentary basins, hydrothermal activities, and dissociation of gas hydrates (Etiope et al., 2019). Methane gas can be emitted by several natural and anthropogenic sources into the atmosphere (Weber et al., 2019; Oppo et al., 2020). Methane has multiple natural sources including marine cold seeps and gas hydrates (Morales et al., 2017). The sea floor is assumed to be the major source of this methane, where it is produced microbially in anoxic sediments or released from geological reservoirs at hydrocarbon seeps and degrading gas hydrate deposits (Weber et al., 2019; Oppo et al., 2020). Methane is available as free gas and gas hydrate within the Arctic Ocean sediments (Yao et al., 2020).

1.1.1 Formation of Methane in the subsurface.

The methane cycle starts with high primary biological productivity where large amounts of organic matter (mainly planktons) are deposited over millions of years in the seabed along the edge of the continents (Selley, 2014). As the organic materials sink and accumulate on the seafloor, it becomes buried under layers of sediments. Anaerobic microbes (or the effect of pressure and heat in some areas) tend to decompose the organic matter, resulting in the formation of methane (Levin, 2007). Methane formed within the sediment can be squeezed upward by the subduction of oceanic plates under the continental margins (Levin, 2007). Methane can occur in solid form (hydrate) at high pressure and low

temperatures in the deep-sea (Selley, 2014). The hydrates form by the movement of methane gas upward in the seabed along faults and cracks or low-permeability stratigraphic pathways. Contact with cold water within the seabed results in crystallisation, hence methane becomes trapped and embedded in water molecules, forming solid ice (Levin, 2007; Selley, 2014).

1.1.2 Source Depth of methane.

Methane seeps have been reported from the shallow subtidal zone to the deep Ocean trenches, at depths between 15 m to more than 7800 m (Levin, 2007). Methane produced at shallow depth due to microbial degradation at temperature lower than 50^{o}c is called microbial methane (Milkov and Etiope, 2018; Selley, 2014), and it is the principal source of gas seeping at the seafloor during the last 100 million years (Oppo et al., 2020). On the other hand, methane produced at greater depths due to burial of organic matter at temperatures greater than 50^{o}c is called thermogenic methane (Milkov and Etiope, 2018; Selley, 2014), which may constitute seepage where deep hydrocarbon source rocks and reservoirs are connected to the surface through conduits such as faults and fractures (Oppo et al., 2020). Microbial methane migrates short distances to the seafloor while thermogenic methane generally migrates longer distances from deeper reservoirs and source rocks through faults to the seafloor (Miyajima et al., 2020).

1.2 Foraminifera as A Proxy for Paleo-Methane Emissions.

Foraminifera are single-celled eukaryotic creatures that live primarily in marine habitats. These creatures feed on phytodetritus and prokaryotes, consuming metazoan tissues (Armstrong & Brasier 2005). As a result, it has been suggested that aerobic methanotrophic bacteria could provide a supplementary food supply for these species, allowing them to survive in cold seeps (Panieri, 2006; Rathburn et al., 2003). Foraminifera have been employed as a proxy for paleo-methane emissions, primarily because of their stable isotopic signature (Millo et al., 2005a, 2005b; Panieri et al., 2012, 2014; Torres et al., 2010; Dessandier et al., 2019). Foraminifera are significant because their fossil tests are being used in biostratigraphy, paleoenvironmental studies, and isotope geochemistry. As they are found in almost all marine sediments, often in large, well-preserved, wide, and varied assemblages, they are the most studied group of fossils on the planet (Armstrong & Brasier, 2005).

Several studies have been carried out to investigate the assemblages and stable isotope composition of foraminifera sampled at methane seeps from various geographical locations, including the Barents Sea (Argentino et al., 2021); western offshore Svalbard (Panieri et al., 2016; Consolaro et al., 2018), Mediterranean Sea (Panieri, 2006), California Margin (Rathburn et al., 2000), Gulf of Mexico (Hill et al., 2003), and offshore New Zealand (Dessandier et al., 2019). Foraminiferal calcite could be used as a tool to investigate the history of seafloor methane seepage in this critically cold Arctic environment (Panieri et al., 2016). Even though sites with high methane concentrations have a lower number and diversity of agglutinated species, all these studies found that cold seeps have no endemic species. (Dessandier et al., 2019 and reference therein).

Studies on foraminifera from Vestnesa Ridge have shown that the precipitation of methane-derived authigenic carbonate (MDAC) can significantly affect the stable isotopic composition of foraminifera from cold seeps (Consolaro et al., 2015; Panieri et al., 2016; Schneider et al., 2018; Dessandier et al., 2019). As a result, having a strong understanding of species ecology should help researchers better understand how foraminifera can live and record methane seepage episodes (Dessandier et al., 2019).

Foraminifera tests can be abundant in marine sediments; they account for over 55 percent of Arctic biomass and over 90 percent of deep-water biomass in the modern ocean (Armstrong & Brasier, 2005). Foraminifera can record and preserve changes in marine environmental conditions through the mineralization build up on their calcitic tests (Panieri et al., 2016; Schneider et al., 2018; Dessandier et al., 2021). The overgrowth of methane-derived authigenic carbonate (MDAC) on and in foraminiferal tests has been shown to explain the majority of the negative $\delta^{13}C$ excursions reported in cold seeps (Panieri et al., 2016). The $\delta^{18}O$ isotope composition of the tests give information about the ocean's past temperature (Panieri et al., 2016; Dessandier et al., 2020; 2021) and the $\delta^{13}C$ isotope compositions provide information about the dissolved inorganic carbon (DIC) in the water in which they calcified (Panieri et al., 2016). Benthic Foraminifera can be associated with methane seepage sites, research has shown that their calcitic tests can incorporate the negative $\delta^{13}C$ values of dissolved inorganic carbon got from the oxidation of methane in the pore space of surrounding sediments (Consolaro et al., 2015).

At cold seeps, methane-derived authigenic carbonates can form in a variety of shapes, including slabs, crusts, nodules, chimneys, and pipes, and have typical negative $\delta\ ^{13}C$ values

(Consolaro et al., 2015). At the interface between upward-moving methane and downward diffusing sulphate in the sediment pore water column is the SMTZ (Sulphate Methane Transition Zone), where methane is oxidized anaerobically as follows (Boetius et al., 2000; Panieri et al., 2016):

$CH_4 + SO_4^{2-} \longrightarrow HCO_3^- + HS^- + H_2O$ (Equation 1)

The sulphate-methane transition zone (SMTZ) is a zone at or variable depth beneath the seafloor where microbial co-metabolism balances the upward flux of methane with the downward flux of sulphate (Schneider et al., 2018). The SMTZ can migrate vertically through the sediment as the methane flux changes (Panieri et al., 2016; Schneider et al., 2018). At high-flux seep sites, the SMTZ is often very shallow, and methane may escape directly into the water column, where methanotrophic aerobic microbes in the water column consume most of the methane emitted at the seafloor (Consolaro et al., 2015). As a result, planktonic foraminifera do not typically record negative methane-derived $\delta^{13}C$ values in their tests when they are in the water column, but when they die and sink into the sediment, they could be altered by MDAC which precipitate on them. Indeed, both planktonic and benthonic foraminiferal tests can be altered by the precipitation of methane derived carbonates around their shells.

The HCO_3^- bicarbonate ions produced from the previously mentioned reaction (Equation 1) go into further reaction with the Ca/Mg ions that are available in the sediment pore waters to produce $Ca/MgCO_3$ (Panieri et al., 2016) - a form of precipitate, which settles as well as build on the existing foraminiferal tests. At methane seeps, foraminifera tests are suitable templates for authigenic Mg-calcite precipitation, according to Panieri et al. (2017). These $Ca/MgCO_3$ are low in ^{13}C isotope value. Depleted value of $\delta\ ^{13}C$ is an indication of seepage as well as cementation of MDAC on the foraminiferal tests (Panieri et al., 2016). Benthic foraminifera also show slight depleted negative $\delta\ ^{13}C$ values as low as -5.6 ‰ when they feed on methanotrophic microbes at the seafloor by incorporating ^{13}C-depleted C from that biomass into their tests while metabolic active (Panieri, 2006; Rathburn et al., 2003; Schneider et al., 2018). Generally, foraminifera that feed on microbial mats at cold seeps have slightly negative values of $\delta\ ^{13}C$ values ranging from -1.5 to -5 ‰ (Dessandier et al., 2019).

1.3 Objective of the Study

This study aims to isolate foraminifera from the sediment samples of the gravity core, push core, and blade core collected from the Svyatogor Ridge (Fig.1), Arctic Ocean during the CAGE21 Expedition and analyse their stable Carbon and Oxygen isotopic composition for reconstructing the history of seepage in the area. The isotope geochemistry ($\delta^{13}C$ and $\delta^{18}O$) of the foraminifera tests, sediment geochemistry (TOC, TN, $\delta\ ^{13}Corg$, $\delta\ ^{15}N$, Carbon, and Nitrogen), and chemical compounds of the sediments (elemental ratios from XRF analysis) were the proxies used to reconstruct the episode of seepage in the area and characterize the sources of organic matter in the sediment.

1.4 Study Area and Geological setting: The Svyatogor Ridge, Arctic Ocean

The Svyatogor Ridge is in the high-Arctic Svalbard archipelago at the northeastern part of the North Atlantic continental shelf margin (Johnson et al., 2015) in the Fram Strait (Waghorn et al., 2018) in the Arctic Ocean. It is a submarine ridge to the west of Svalbard. It is an elongated, sedimented active mid-ocean ridge situated on the northwestern flank of the Knipovich Ridge and south of the Molloy Transform Fault (MTF) (Waghorn et al., 2018). The Svyatogor Ridge is about 80km south of the Vestnesa Ridge, both ridges were part of the same ridge complex until they were demarcated by the Molloy Transform Fault (Johnson et al., 2015). Movement on previously sedimented detachment faults has resulted in the formation of sedimentary faults on the Svyatogor Ridge (Waghorn et al., 2020). It is an active mid-ocean ridge made of contouritic sediment which spans 46km and approximately 5km in length and width respectively (Waghorn et al., 2020). It hosts extensive gas hydrates and fluid flow systems (Waghorn et al., 2018; 2020) and therefore an active methane seepage site. It has gas hydrate systems on its flanks (Johnson et al., 2015).

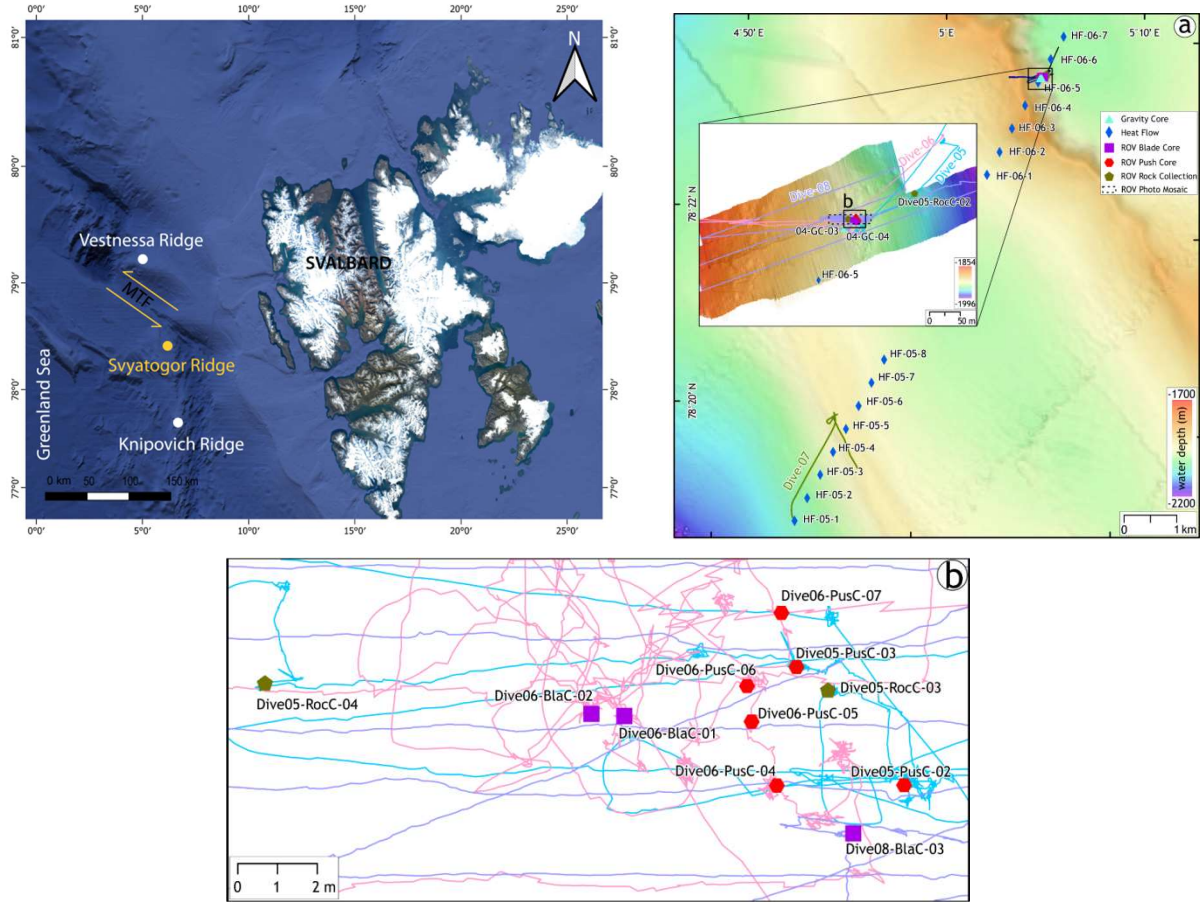

Fig.1: Left panel: map of the study area (modified from Google maps).
Right panel: (a). Position of gravity core (04-GC-03)
Lower panel: (b). Position of push core (dive06-Pusc-07) and blade core (dive08-Blac-03)

Waghorn et al. (2020) suggested that abiotic methane may contribute to the gas hydrate system on the western Knipovich Ridge flank of the Svyatogor Ridge. It is an actively rifting environment (Waghorn et al., 2018). The associated faults act as conduits for fluid escape or seepage routes (Waghorn et al., 2020). Shallow gas accumulations have been found on Svyatogor Ridge, as well as a high Bottom Simulating Reflector indicating a gas hydrate and underlying free gas system, and fluid flow channels to the seafloor that end in pockmarks (Waghorn et al., 2018).

1.5 The Use of Proxies

According to the National Centres for Environmental Information, Proxy data in palaeoclimatology are physical properties of the environment that have been retained and can be used in place of direct measurements. We cannot see the crucial variables in a system that

no longer exists to reconstruct the history of methane emission in the past; instead, we can employ proxies as qualitative or semiquantitative descriptors for a desired but unobservable environmental variable (Yao et al., 2020). Proxies are evidence, indications, signs, and records of events. Methane seepage history can be reconstructed by using certain proxies preserved in the geological record (Yao et al., 2020). Stable isotopes of oxygen ($\delta\ ^{18}O$) and carbon ($\delta\ ^{13}C$) measured on foraminiferal tests, organic substances (C/N, TOC), chemical compounds of sediment (Ca and Ba peaks of XRF logs as proxies for carbonate and barite enrichment in the sediment), and shells of macrofaunal are indeed the proxies employed in this study.

1.5.1 Foraminifera

Foraminifera are single-celled marine microorganisms that live in two modes: planktonic and benthic. Planktonic forms are found floating in the water column and they sink to the bottom sediments when they die. Benthic foraminifera live on the surface of a submerged substrate as epibenthic (epifaunal species) and within the sediments as endobenthic (infaunal species). Infaunal species are often tolerant of low oxygen content and deep infaunal are the most tolerant while epifaunal species are not tolerant of oxygen deficiency but require high oxygen levels (Armstrong & Brasier, 2005). The ratio between the number of epifaunal species and the number of infaunal species are often an indication of the level of oxygenation of the environment (Armstrong & Brasier, 2005). Benthic foraminifera are often well conserved and can be found in large numbers in small sediment samples. Most species are responsive to changing environmental variables such as water temperature, salinity, and water currents (Armstrong & Brasier, 2005). These changes are recorded during the development of their tests as they utilise the components in their surroundings at the time they lived, making them excellent paleoenvironment markers (Panieri et al., 2016; Schneider et al., 2018; Dessandier et al., 2021).

1.5.2 Stable Isotopes of Carbon and Oxygen of the Foraminifera

Stable isotopes are non-radioactive atoms of the same element that have the same number of protons but a different number of neutrons. Because of the electronic configuration, their chemical properties are the same, but their physical properties are not.

Most naturally occurring elements consist of more than one stable isotope. These elements have been the subject of geochemical investigations for many decades and are termed the *traditional stable isotopes*. Since foraminifera make their tests from $CaCO_3$, the isotopic proportions of Carbon (C), Calcium (Ca), and Oxygen (O) are retained during their creation. The salinity and temperature of paleoenvironments can be determined by analysing the ratio between $^{13}C/^{12}C$ and $^{18}O/^{16}O$. Carbon stable isotopes include the lesser ^{12}C and heavier ^{13}C. Because photosynthetic organisms prefer the lighter ^{12}C, ^{12}C is stored away in living organisms and buried organic matter during high primary production. As a result, the atmosphere and oceans are enriched in ^{13}C and deficient in ^{12}C, resulting in high $\delta^{13}C$ ($^{13}C/^{12}C$) levels. This is shown in foraminifera tests, which use enriched ^{13}C water to determine if the environment is adequate for biological productivity as seen in Figure 2 below. The δ ^{13}C of calcite in benthic foraminiferal reflects that of the dissolved inorganic carbon (DIC) in the oceans where they are calcified (Panieri et al., 2016).

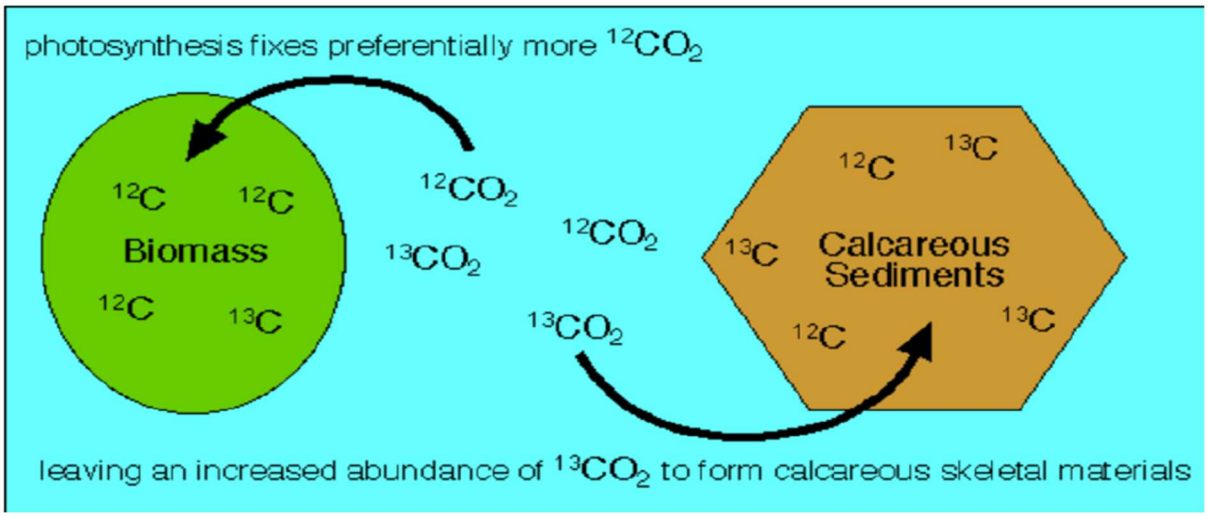

Fig.2: Simple representation of living organisms using ^{12}C for photosynthesis, resulting in ocean water being enriched with ^{13}C, which is absorbed in sediments, as well as tests and shells of micro and macrofauna (Columbia University).

^{16}O, ^{17}O, and ^{18}O are oxygen isotopes, with ^{16}O being the lightest and ^{18}O being the heaviest. Because the lightest isotope ^{16}O requires less energy to evaporate than ^{18}O when water molecules are produced, $\delta^{18}O$, which reflects the ratio of $^{18}O/^{16}O$, will be high during cold temperatures because the light ^{16}O would have been evaporated and locked in ice (Fig.3) (Columbia University). Due to the large levels of $\delta^{18}O$ in ocean waters, this is documented in foraminifera tests, which utilize seawater to form and can be quantified using an isotope ratio mass spectrometer.

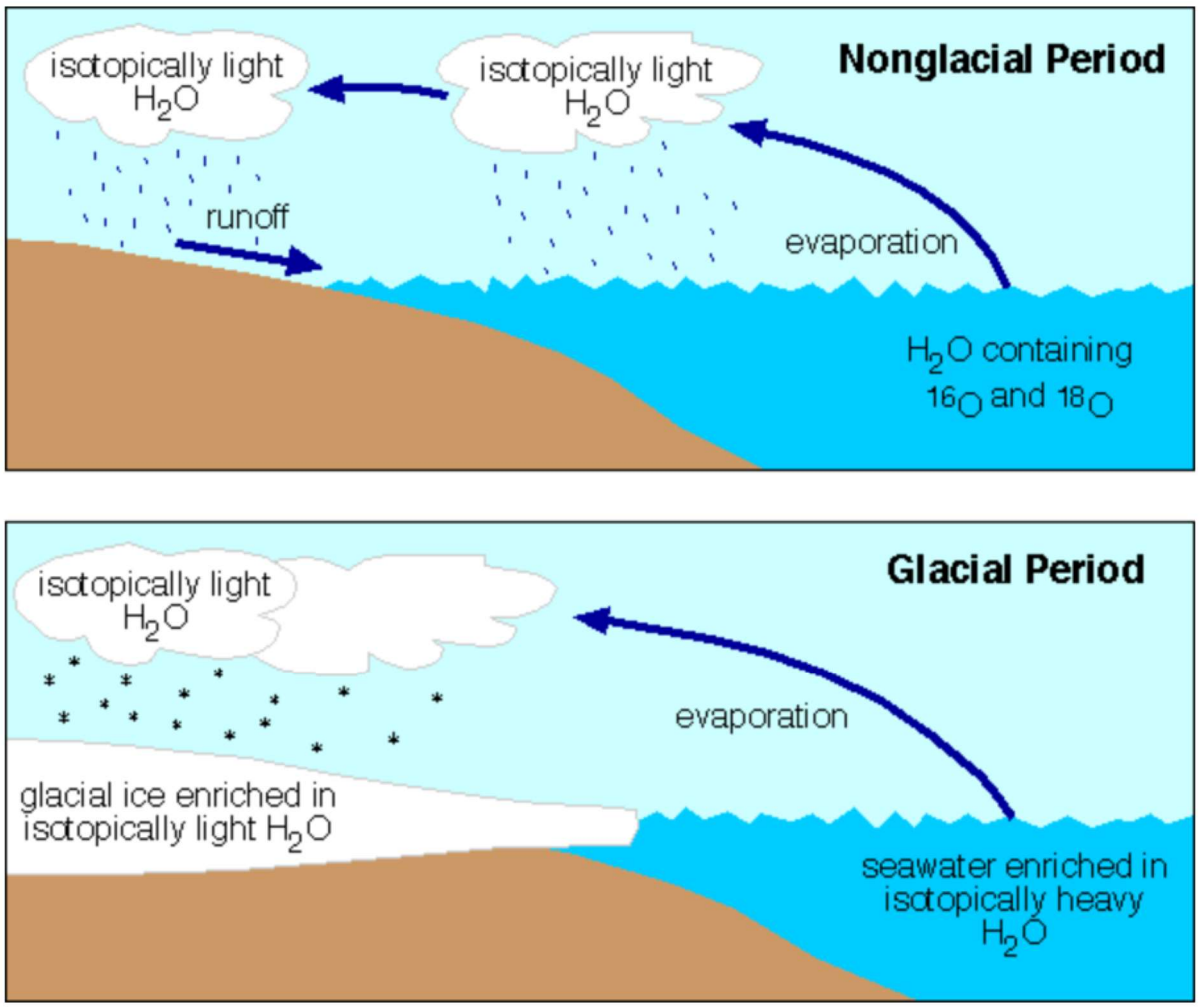

Fig.3: During nonglacial periods, light ^{16}O is evaporated and returned to the ocean, whereas during glacial periods, light H_2O is retained in ice and the ocean is enriched with heavy ^{18}O. (Columbia University).

1.5.3 Organic Compounds of Carbon and Nitrogen

The volume and kind of organic matter in lake and ocean sediments contribute to paleoenvironmental and paleoclimatological records. Only a small percentage of the initial aquatic biological matter survives the destruction and change that occurs during sinking and sedimentation (Meyers, 1994). Nonetheless, source and paleoenvironmental information are preserved in the molecular, elemental, and isotopic compositions of organic matter. C/N- and $\delta^{13}C$-values of total organic matter appear to preserve paleoenvironmental information over multi-Myr time scales (Meyers, 1994). Carbon isotopic ratios, as well as the C/N, can be used to differentiate between marine and continental plant sources of sedimentary organic matter, as well as to identify organic matter from different species of land plants (Meyers, 1994). In this case, the $\delta^{13}C$ is derived from the sediment below the seafloor and it is measured as:

δ^{13}Corg (‰) = [(^{13}C/^{12}Corganic/^{13}C/^{12}C$_{V-PDB-Std}$) - 1] X 1000).

Nitrogen is a critical nutrient in the marine environment, and its measurements help us understand the past and present of the marine nitrogen cycle (Meyers, 1994). The two stable isotopes of nitrogen are ^{15}N and ^{14}N, and the ratio ^{15}N/^{14}N is utilized in the equation below to represent δ^{15}N.

δ^{15}N (‰) = [(^{15}N/^{14}Nsample/^{15}N/^{14}Natm, $_{N2}$) - 1] X 1000)

The nitrogen cycle is controlled by the nutrients that phytoplankton consumes and produces. Phytoplankton is a type of high-quality organic matter that degrades further once it reaches the seafloor. As a result, δ^{15}N can be used as a proxy for nutrient use in relation to phytodetrital productivity and breakdown (Meyers, 1994).

1.5.4 Chemical Compounds of Sediments

X-ray fluorescence (XRF) analysis of sediment chemical compounds is a particularly valuable proxy because it is a non-destructive method for determining the elemental composition of sediments. The intensities of single elements are recorded, and the ratios are discussed in the method section. To aid in determining key climatic events, certain elemental ratios were chosen based on literature that indicate grain size, organic matter fluxes, and marine and terrigenous influences.

CHAPTER 2

2. Materials and Methods

This Project work comprises sediments from one Gravity core, one Push core and one Blade core. These cores were collected during the CAGE21_1 (AKMA) Cruise from the Svyatogor Ridge (Fig.1), Arctic Ocean. Details of the cores are given in table 1.

Core ID	Activity	Co-ordinates	Water depth (m)	Recovery (cm)	Comments/ Habitat
CAGE21_1KH04	PusC 7 (Push core)	78.3925 ^{0}N(Lat) 5.0834 ^{0}E (Long)	1928	37	Reference
CAGE21_1KH04	BlaC 3 (Blade core)	78.3925 ^{0}N (Lat) 5.08346 ^{0}E(Long)	1929	21.5	Microbial mat + tubeworm
CAGE21_1KH04	GC3 (Gravity core)	78.3924 ^{0}N (Lat) 5.0825 ^{0}E (Long)	1893	208	

Table 1: Information on sampling stations

The following procedures were carried out on the samples at the Geology Laboratory of the UiT/The Arctic University of Norway:

2.1 X-ray

This procedure provides a radiograph of major features such as lumps of organic matter, ice-rafted deposits, shell fragments, plant root structures, and voids or other types of intrusions within the sediment core. Visual descriptions, X-ray scanning (GeoTek MSCL-XR3.0), and photography (Jai L-107CC 3 CCD RGB Line Scan Camera) were used to describe the cores. X-ray of 130KV and 370µA was sent through the 3 sections of the gravity cores to get images from the cores.

2.2 Magnetic Susceptibility

This involves the use of the Multi-Sensor Core Logger (MSCL). MSCL systems extract high-resolution (typically 1 cm to 10 cm downcore spacing) geophysical and geochemical data from sediment and rock cores in a fast and non-destructive manner. MSCL systems' high-quality multi-parameter stratigraphy enables facies classification and soil/rock typing before, or in addition to, a visual description. Prior to destructive laboratory testing or visual logging, an MSCL dataset provides critical information about core heterogeneity or homogeneity. The Multi-Sensor Core Logger measures the amount of magnetically susceptible material in the sediment. Such sensors generate a stream of precise, accurate measurements with spatial resolutions as low as a few mm, which scientists and engineers can use both for their intrinsic values and as proxies for changes in lithology, texture, or sedimentary origin. Magnetic Susceptibility (MS) and Bulk Density (BD) of the 3 sections of the gravity cores were measured using the GeoTek Multi-Sensor Core Logger at sampling intervals of 1 cm and count time for Gamma at 10 seconds.

2.3 X-Ray Fluorescence (XRF) analysis of the gravity core

X-ray fluorescence is a non-destructive analytical technique that the 3 sections of the gravity cores were subjected to reveal elemental composition. The analyzer obtains elemental abundance from sediment and rock core surfaces. The XRF analyzer does this by measuring the fluorescent X-ray emitted from the sample when excited by a primary X-ray source. XRF is an excellent technique for qualitative and quantitative analysis of the elemental composition of a sample because different elements contained in the samples have distinct characteristics of fluorescent X-rays. Geochemical data from the gravity core was collected in 1 cm intervals using an Avaatech XRF Core Scanner with the following settings: down-core slit size 10 mm; cross-core slit size 12 mm; 10 kV, 1000 mA, no filter, and 10 s measuring time per step; 30 kV, 2 mA, Pd-thick filter, and 20 s measuring time per step; and same settings but 50 kV and 20 s measuring time per step with Cu-filter for barium. To prevent contamination of the XRF measurement unit and desiccation of the sediment, the split core surface was covered with 4 mm thick SPEXCerti Prep Ultralene1 foil. The raw data was processed using the WinAxil program.

Scanning entails hitting the sediment with high-energy X-rays from a source, which ionizes the atoms and causes an electron from the inner shell to be ejected. Almost instantly, an electron from the outer shells falls in and takes its place, releasing radiation that is detected by a detector. Because each element has its own unique energy, the elemental makeup of sediment samples may be measured using the radiation that has been released. Elemental ratios, rather than single element intensities, have been employed as environmental indicators because they are suited for correlation and have been used by various writers. Two-element ratios also lessen the consequences of down-core changes (Schneider et al., 2018). The XRF scanning method can accurately assess Ca (Calcium), Fe (Iron), and Ti (Titanium), which were employed in this investigation, as well as Zr (Zirconium), Rb (Rubidium), Br (Bromine), and Cl (Chlorine). For instance, many studies have used Ti and Ca to determine terrigenous and marine constituents; Ti is restricted to lithogenic sediments and is resistant to diagenetic processes while Ca measures the biogenic carbonate abundance such as foraminiferal tests or inorganic MDAC precipitates (Schneider et al., 2018). Hence, the Ca/Ti ratio can be used as a proxy to follow variations in biogenic and lithogenic sedimentation. Because Zr is found in coarser particles than Rb, the Zr/Rb ratio is a well-known proxy for grain size (Schneider et al., 2018), and it rises as the particle size of the sediment increases (Yao et al., 2020). And as a proxy for organic matter, the Br/Cl ratio was employed (Ziegler et al., 2008). Ba/Ti ratio is an indication of barite minerals associated with the paleo- or modern position of the sulfate-methane transition zone (SMTZ) (Yao et al., 2020).

2.4 Sampling of the Gravity Core, Push Core, and Blade Core

This involved taking some sediment samples from the cores for various analyses. The gravity core GC3 has a length of 214 cm, and it was cut onboard into 3 sections: GC3_1, GC3_2 and GC3_3. GC3_1 has a length of 0 – 58 cm, GC3_2 has a length of 58 – 113 cm and GC3_3 has a length of 113 – 214 cm. Each of the 3 sections of the gravity cores was split longitudinally into two halves, with one half as the archive core for possible future sampling, and the other half as the working core where samples were taken for various analyses. The gravity cores were sampled from the top to bottom. The gravity core GC3_1 was sampled at 10 cm interval, GC3_2 at 5 cm interval and GC3_3 at 10 cm interval. The first 25 to 30 cm length of GC3_3 was not sampled initially due to the shell fragments content but later

sampled at 1cm interval. The Blade core has a length of 20 cm, and samples were taken at each cm starting from the seafloor (0 cm). The Push core has a length of 42 cm and samples were taken at intervals of 1 cm, starting from 0 cm. These sediment samples were completely freeze-dried in small bags in the freeze dryer. This was done to prevent sediment samples from melting.

2.5 Organic Compound Analysis

Portions of sediments samples were taken from the freeze-dried sediment samples for grinding. These samples were ground in 2mL Eppendorf tubes with a round bottom using one 7 mm steel ball and run at 15 Hz for 5 minutes. The ground sediment samples were transferred into glass centrifuge tubes. 5 mL of 6 M HCl was added to the ground sediment samples in the glass centrifuge tubes. This was done to dissolve the inorganic carbon content of the sediment samples. After 48 hrs, the acid was discarded, and 5 mL of distilled water was added and centrifuged. The water was discarded. The adding of distilled water and discarding it was done repeatedly until the pH was 6.5. Sediment samples with dissolved inorganic carbon content were dried completely at 50^0c. From the dried sediment samples with dissolved inorganic carbon, 18 to 22 mg samples were weighed in tin cupsules and were subjected to the combustion reactor of the Thermo Scientific Flash 2000 HT Elemental Analyser with the required amount of oxygen (Thermo Fisher brochure). The sample was subsequently burned at 1020°C, with the resulting gases transferred into a reactor by helium flow, where carbon was transformed to CO_2 and nitrogen to N_2. These gases were then passed via a water trap to remove H_2O, then a (Gas Chromatography) GC column to separate the carbon and nitrogen, which could then be supplied into the Isotope Ratio Mass Spectrometry, IRMS (Fig.6). The IRMS measured the abundance of ^{13}C and ^{15}N isotopes in the individual particles by comparing them to the Vienna Pee Dee Belemnite (VPDB) for carbon and relative air for nitrogen through the process described below (Fig.4). The atomic mass-weighted ratio of TOC and TN was used to compute the C/N atomic ratio, which was C/N = (TOC/12.011)/(TN/14.007).

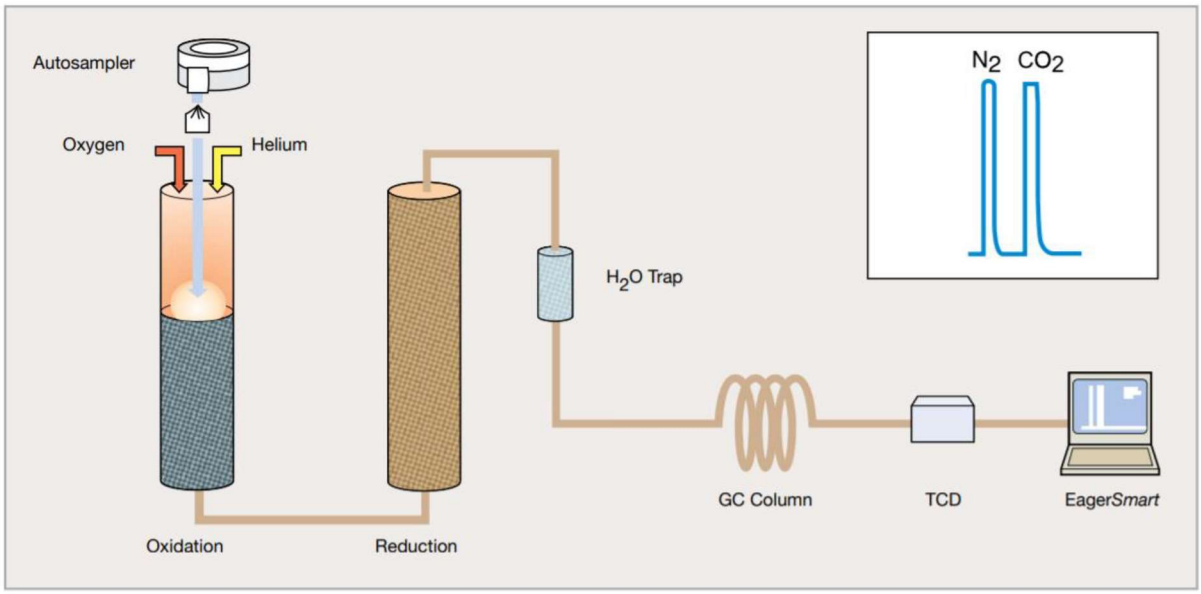

Fig.4: Process of the elemental analyzer Flash 2000 (Thermo Fisher Brochure)

2.6 Micropaleontological Analyses

Portions of the freeze-dried sediment samples collected from the gravity, push and blade cores were weighed and wet-sieved using the 63 and 125 µm sieve fractions. A total of 108 samples have been processed. The residues were dried at 40^0c. Benthic and planktic foraminifera were picked using a binocular microscope from the 125 – 500 µm size fraction, , and identified to species level for isotopic analysis. A number from 5 to 15 specimens have been selected. *Neogloboquadrina pachyderma*, a planktonic foraminiferal species and *Cibicides wuellerstofi,* a benthonic foraminiferal species were the most dominant in the sediment samples and appear in most of the samples. Some of the samples in the sediment cores were barren, then only 79 of the 108 samples processed contain abundant and representative foraminifera that could be measured.

2.7 Stable Isotope Analysis

Neogloboquadrina pachyderma and *Cibicides wuellerstofi* were selected to perform isotopic analysis because of their abundance and dominance in the sediment samples and in the Arctic Ocean. *Neogloboquadrina pachyderma* is the planktic species and *Cibicides wuellerstofi* is the benthic species. The foraminifera recovered in the slides during picking were carefully moved to small glass vials (Fig.5) ensuring that all foraminifera sat at the

bottom of the vial so that the phosphoric acid could reach it. Vials were labelled with numbers matching to their interval in the cores and then analyzed at the Stable Isotope Laboratory, Centre for Arctic Gas Hydrate, Environment, and Climate in the Department of Geosciences at The Arctic University of Norway in Tromsø (UiT, Tromsø). The Thermo-Fisher MAT253 IRMS with a Gasbench II, which is used to read $\delta^{13}C$ and $\delta^{18}O$ concentrations in carbonates, was employed in this study. The Gasbench II is first used to generate CO_2 from the specimens' carbonate tests.

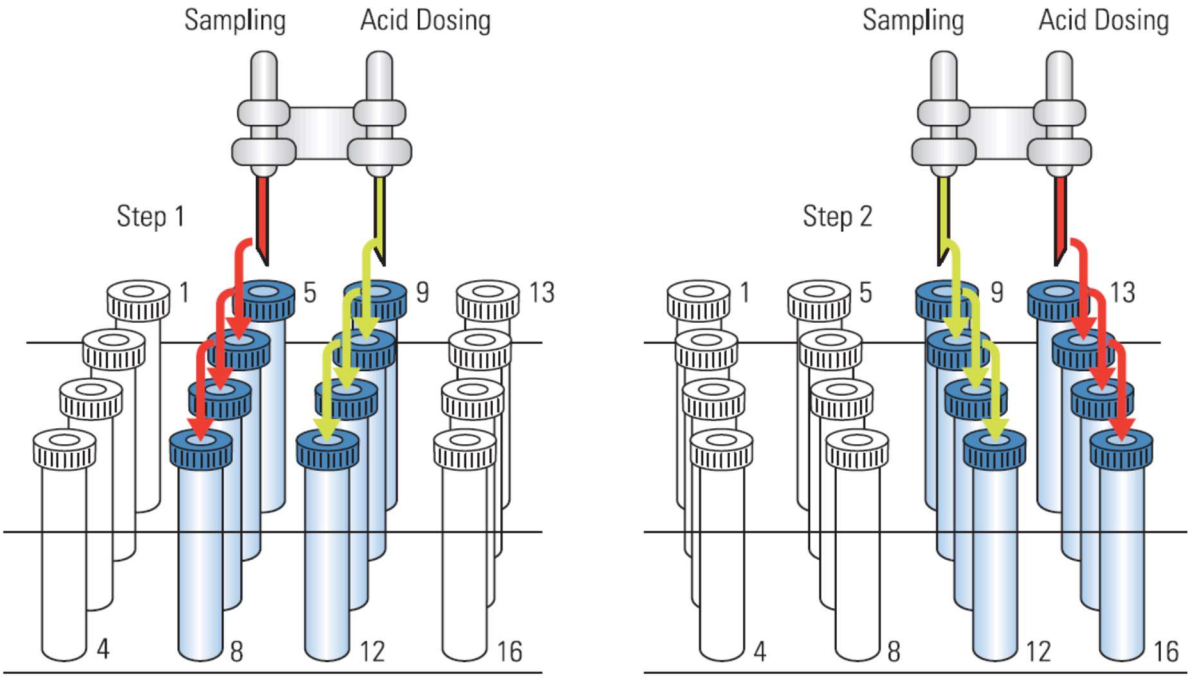

Fig.5: Kit for Carbonate Reaction (Thermo Scientific GasBench II Brochure)

This is accomplished by dissolving the foraminiferal tests, a procedure known as 'acid bath,' which entails using a microliter pump to inject phosphoric acid into the sample vials illustrated in Figure 5 and yields a precision of 0.08‰ for $\delta^{18}O$ and 0.06‰ for $\delta^{13}C$. (Thermo Scientific GasBench II Brochure).

The phosphoric acid (H_3PO_4) dissolves the calcium carbonate ($CaCO_3$), the substance that forms the foraminifera tests, leading to the emission of a gas containing calcium phosphate ($CaHPO_4$), water (H_2O), and carbon dioxide (CO_2), as given in the equation below.

$$CaCO_3 + H_3PO_4 \longrightarrow CO_2 + H_2O + CaHPO4$$

The gas in the vial is then diluted with helium (He), which displaces it and allows it to flow upward out of the vial and into a diffusion trap, where the water is removed. The gas then passes through a loop that aliquots the sample and separates the molecules on the gas chromatograph column (GC) (Thermo Scientific GasBench II Brochure). The remaining separated particles are transported to the isotope ratio mass spectrometry (IRMS) (Fig.6) after a reference gas is injected to allow correct referencing of the sample to isotopic standards.

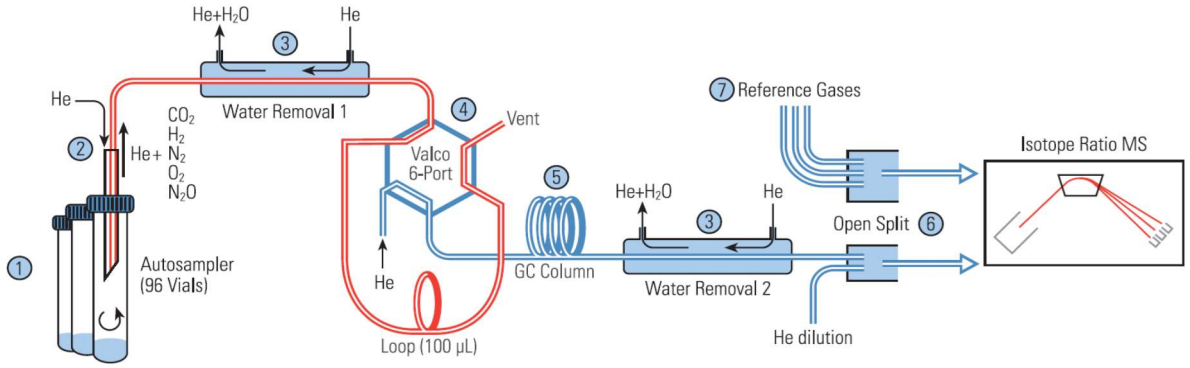

Fig.6: Scheme for Gasbench (Thermo Scientific GasBench II)

The carbon or oxygen particles enter the Thermo-Fisher MAT253 IRMS, where they are ionized by an ion source, resulting in a positive charge that is driven forward by an electric field. The particles then approach a magnetic field, where their propulsion path is deflected based on their mass, with heavier particles deflecting less and lighter particles deflecting more (Fig.7). This process divides elements into isotopes of different masses, such as carbon (C) into ^{12}C, ^{13}C, and ^{14}C, and oxygen (O) into ^{16}O and ^{18}O. The particles then impact a detection plate, which measures an isotope's abundance. Figure 7 below shows the inner working of the Thermo Fisher.

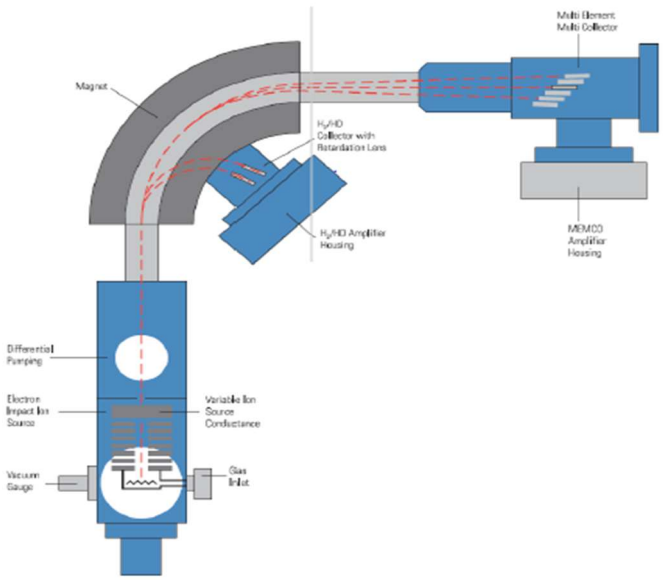

Fig.7: Thermo Fisher MAT253 IRMS (Thermo Scientific MAT 253 Brochure)

2.8 Complementary data: pore water data

The data collected for this master's project were integrated with pore water datasets (unpublished) from the same cores. Porewater samples were collected by Dr. Claudio Argentino during AKMA cruise in 2021 on R/V Kronprins Haakon (report on cage.uit.no). The sulfate concentration was measured at TosLab AS in Tromsø via Ion Chromatography. Dissolved Inorganic Carbon (DIC) and its $\delta\ ^{13}C$ composition were measured at Stable Isotope Laboratory-SIL at UiT on a Thermo Scientific Gasbench II connected to MAT253 IRMS (Isotope-Ratio Mass Spectrometer).

CHAPTER 3

3. Results

3.1 Magnetic Susceptibility (MS) and Bulk Density (BD)

The Magnetic Susceptibility (MS) measured on the gravity core CAGE21_1KH04_GC3 (total length of 214 cm) has the least value of 3.30 SI x 10^5 at 66 cm depth and the highest value of 41.34 SI x 10^5 at 97 cm depth (Fig.8). There was a gradual increase in MS from the top of the core to about 52 cm depth, and at 67 cm to 100 cm depth. The MS started decreasing in values from the depth of 53 cm to 66 cm, and from 101 cm to 107 cm depth. The MS value was fluctuating between 9.92 SI x 10^5 and 23.00 SI x 10^5 from the depth of 116 cm to 214 cm.

The Bulk Density (BD) shows similar trend as the MS with depth (Fig.8). It has the highest value of 2.13 gm/cm^3 at 171 cm depth. There was a steady increase in BD from 1.35 gm/cm^3 at depth 18 cm to 1.48 gm/cm^3 at depth 59 cm. There was gradual increase in values between depths 76 cm to 115 cm, and between depths 118 cm to 134 cm.

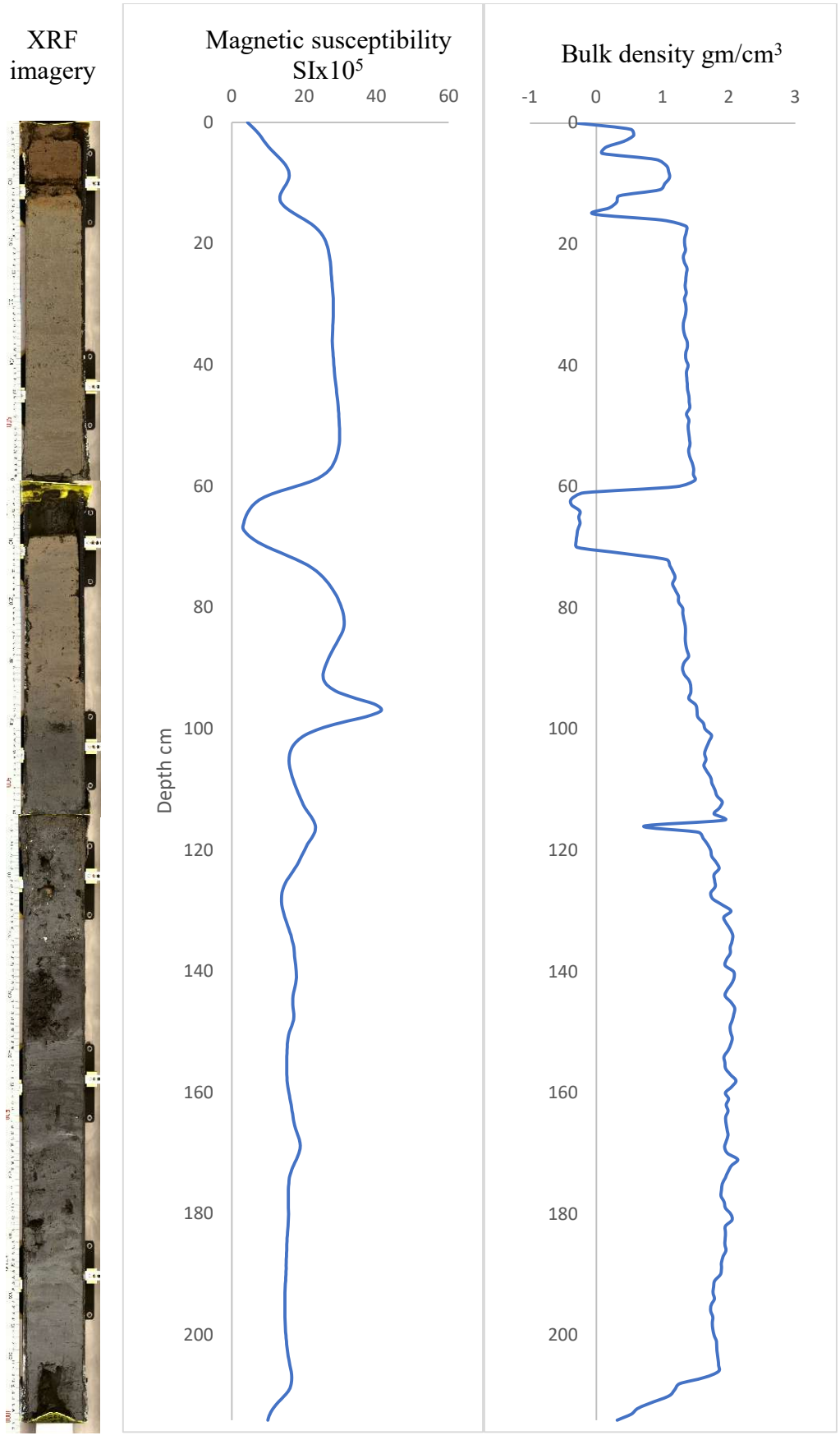

Fig.8: Magnetic susceptibility and Bulk density plotted against depth in the gravity core CAGE21_1KH04_GC3

3.2 X-Ray Fluorescence (XRF)

The X-Ray Fluorescence measured in gravity core CAGE21_1KH04_GC3 shows its elemental composition, and I used two-elemental ratios as they lessen the consequences of down-core changes. Besides, two elemental ratios have been employed as environmental indicators because they are suited for correlation and have been used by various writers. (Schneider et al., 2018). I used the Ca/Ti, Zr/Rb, Ba/Ti and S/Ti ratios. The Ca/Ti ratio shows the variations between biogenic carbonate abundance and terrigenous materials. Zr/Rb ratio is an indication of grain size because coarser particles contain more Zr than Rb. Ba/Ti ratio is an indication of the position of the paleo or modern Sulfate-Methane Transition Zones (SMTZs), where anaerobic oxidation of methane (AOM) processes had occurred or on-going. It peaks immediately above SMTZ. S/Ti ratio is used to complement Ba/Ti ratio as it indicates past and present AOM activity and reduced sediment environment.

The Ca/Ti ratio measured in gravity core CAGE21_1KH04_GC3 shows a decreasing trend right from the top of the core to about 32cm below seafloor (bsf) before it began to increase. It shows a dramatic increase at depths 119 cm and 129 cm. It has low values at depths 60 cm, 105 cm, and 153 cm downward to favour Titanium input. There is no significant change in the proportion of the two elements from depth 160 cm downward (Fig.9).

The Zr/Rb ratio measured in gravity core CAGE21_1KH04_GC3 shows a uniform trend between the top of the core and 58 cm below seafloor (bsf). There is a remarkable negative peak from depth 60 cm to 69 cm and depth 212 cm to 214 cm, which coincide with the empty spaces within the core (Fig.9), so they are artifacts. There is an increase in peak between the depths of 121 cm and 140 cm, with a highest peak at depth 128 cm.

The Ba/Ti ratio in gravity core CAGE21_1KH04_GC3 has multiple peaks at depths 137 cm, 141 cm, 160 cm, and 179 cm while the S/Ti peaks at depths 118 cm, 127 cm and 147 cm (Fig.9).

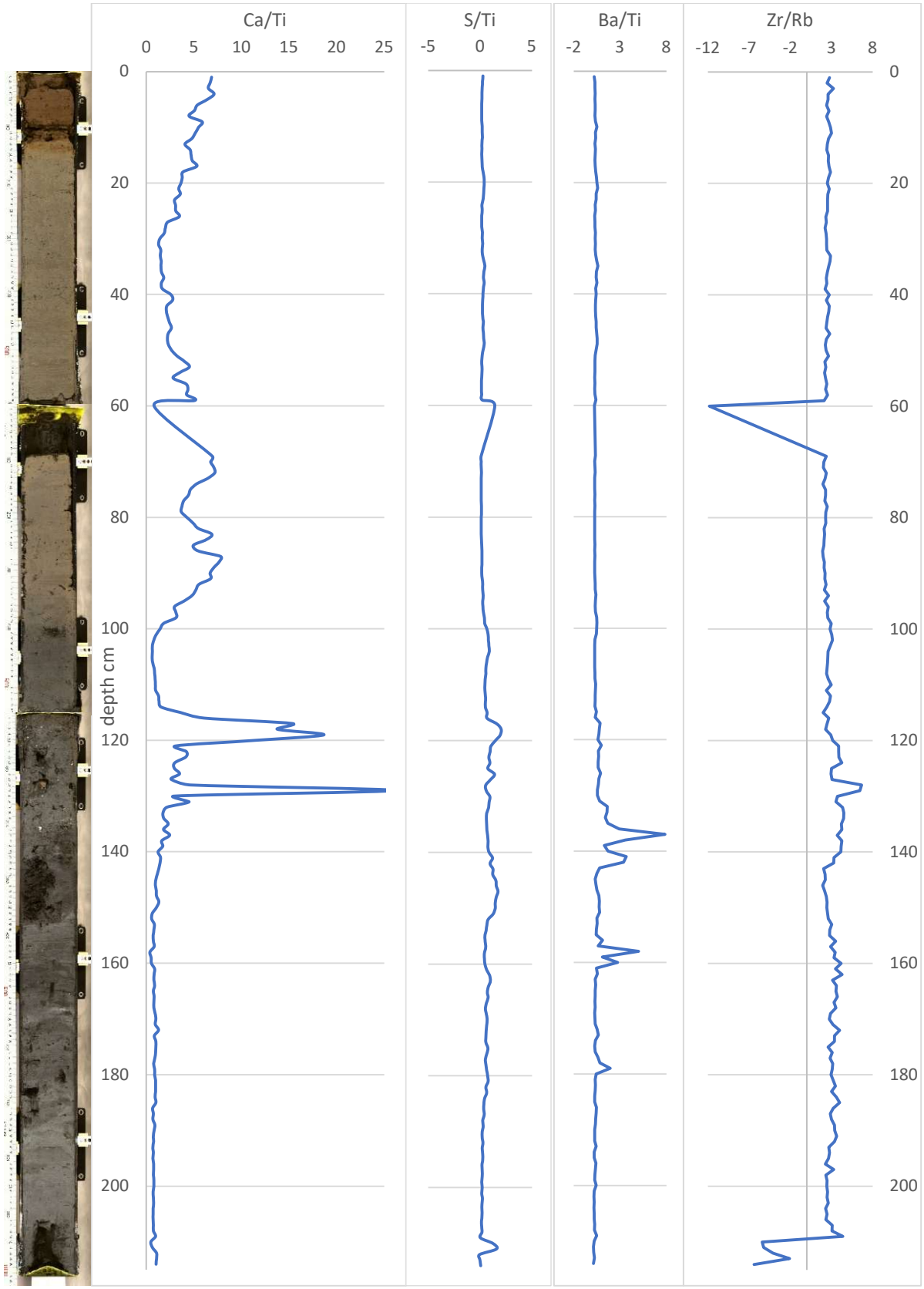

Fig.9: XRF elemental ratios of Ca/Ti, S/Ti, Ba/Ti and Zr/Rb of the gravity core CAGE21_1KH04_GC3 and the XRF imagery along the y-axis.

3.3 Organic Compounds

A total of 117 sediment samples from all the cores were subjected to the carbon and nitrogen isotope analyses to determine the δ $^{13}C_{org.}$, δ ^{15}N, %C and %N. The δ $^{13}C_{org}$ values range between -32.4 ‰ and -23.2 ‰ while the δ ^{15}N values range between 1.2 ‰ and 6.0 ‰. The %C values range between 0.1 and 1.89 while the %N values are between 0.01 and 0.14.

3.3.1 The Push core (CAGE21_1KH04_PusC7)

The δ $^{13}C_{org}$ values are between -27.3 ‰ and -23.2 ‰ while the δ ^{15}N values range between 4.1 ‰ and 5.9 ‰. The %C values are between 0.24 and 0.80 while the %N values range between 0.03 and 0.11. The C/N ratio-values vary between 7.99 and 12.53 (Fig.10).

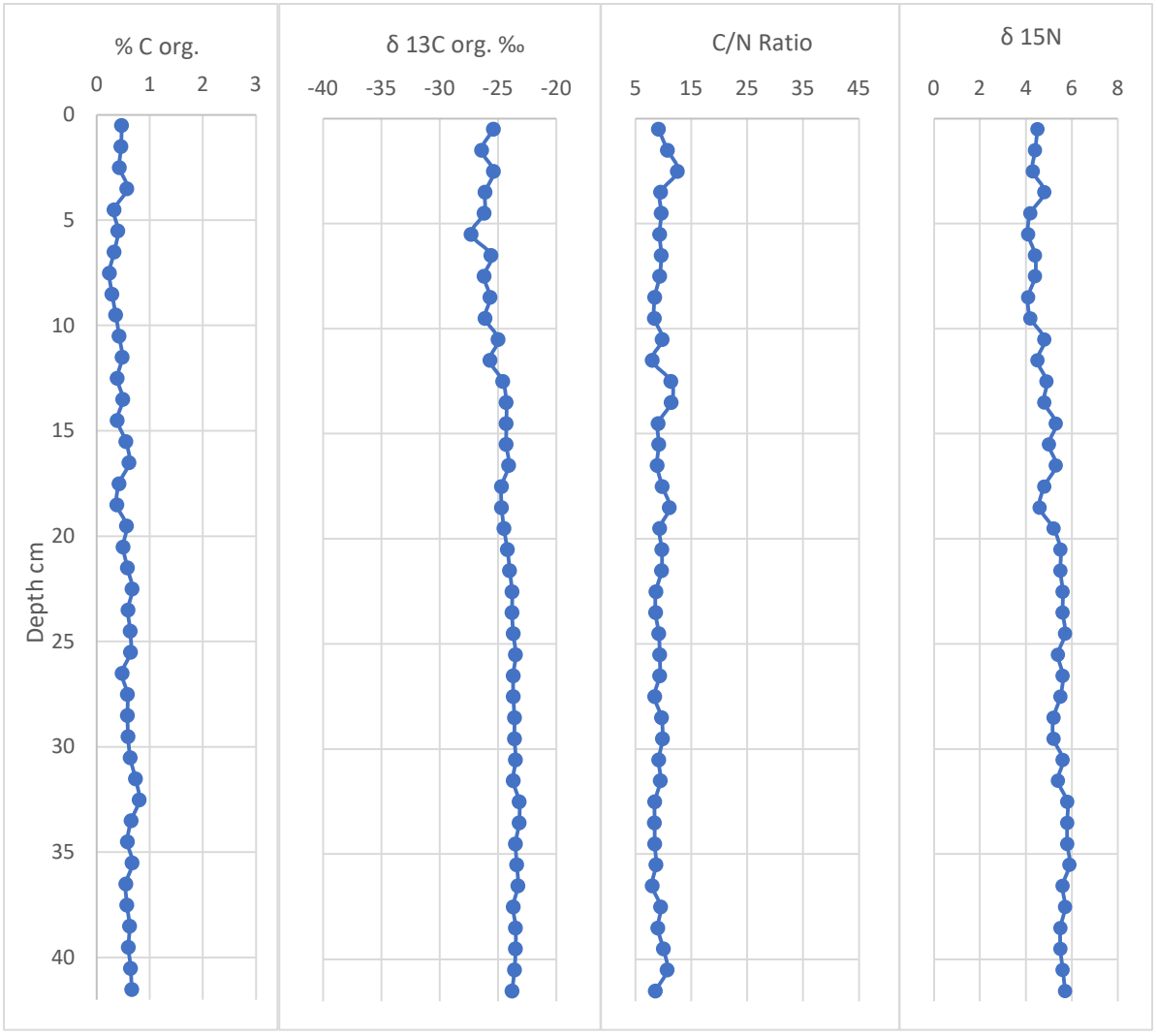

Fig.10: Organic compound plots of depth against %C, δ $^{13}C_{org}$ ‰ and C/N ratio of sediments from the Push core (CAGE21_1KH04_PusC7).

3.3.2 The Gravity core (CAGE21_1KH04_GC3)

The δ $^{13}C_{org}$ values are between -29.4 ‰ and -23.3 ‰ while the δ ^{15}N-values range between 1.7 ‰ and 6.0 ‰. The %C values range between 0.10 and 1.89 while the %N-values are between 0.01 and 0.14. The C/N ratio values vary between 8.74 and 29.15 (Fig.11).

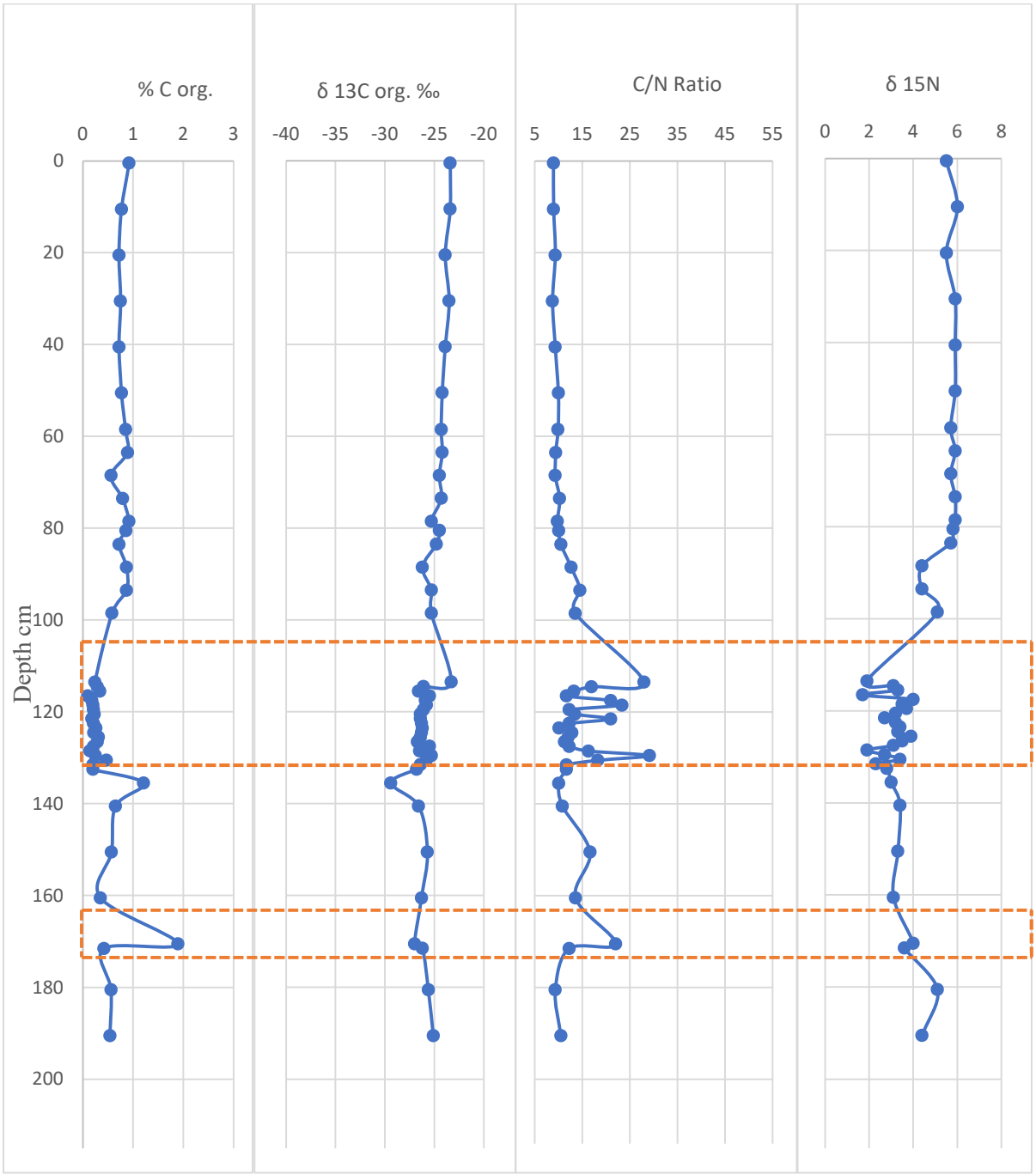

Fig.11: Organic compound plots of depth against %C, δ $^{13}C_{org}$ ‰ and C/N ratio of sediments from the gravity core (CAGE21_1KH04_GC3). Red dotted-line rectangles indicate intervals of terrestrial input into the marine setting based on the C/N ratio values at those intervals.

3.3.3 The Blade core (CAGE21_1KH04_BlaC3)

The δ $^{13}C_{org}$ values range between -32.4 ‰ and -25.4 ‰ while the δ ^{15}N values are between 1.2 ‰ and 4.8 ‰. The %C values range between 0.18 and 0.68 while the %N values range between 0.02 and 0.08. The C/N ratio values vary between 7.77 and 14.77 (Fig.12).

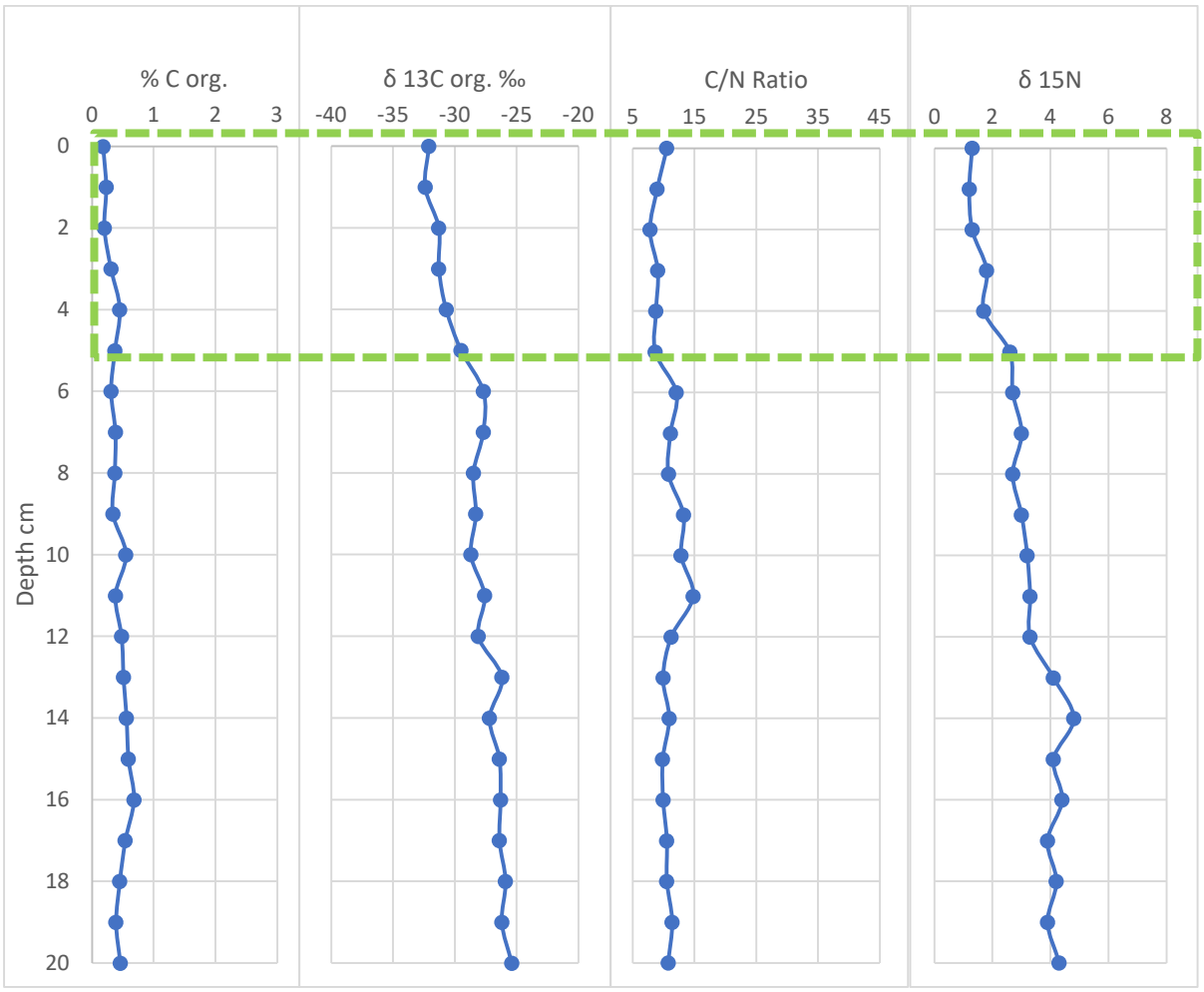

Fig.12: Organic compound plots of depth against %C, δ $^{13}C_{org}$ ‰ and C/N ratio of sediments from the Blade core (CAGE21_1KH04_BlaC3). Green-dotted rectangle indicates methane-influence interval based on the δ $^{13}C_{org}$ ‰.

3.4 Stable Isotopes of Carbon and Oxygen of the Foraminifera

154 samples (68 from the gravity core sediments, 74 from the push core sediments and 12 from the blade core sediments) of foraminifera were subjected to isotopic analysis to produce the δ ^{13}C and δ ^{18}O. The δ ^{13}C values of all the samples range between -12.73 ‰ and

1.26 ‰ while the δ ^{18}O values of all the samples range between -0.53 ‰ and 5.00 ‰. All the sediment intervals from the gravity core (GC3) have enough benthic and planktic species necessary for stable isotope measurements except for 10-11 cm and 20-21 cm intervals where broken and fragmented species of the benthic species were used. 78-79 cm interval lacked the benthic species; intervals from 88 cm to 99 cm and 133 cm downward lacked both species, so no data were collected for these intervals (Fig.13). All the intervals from the push core (PusC_7) have both species apart from 1-2, 2-3, 3-4 and 4-5 cm that lacked both species, therefore no data for these intervals (Fig.14), also intervals 9-10 cm and 10-11 cm lacked benthic species. Majority of the intervals from the blade core (BlaC_3) such as 1, 2, 3, 5, 6, 7, 8, 9, 10, 11, 12, 13 and 14 cm lacked both species, and intervals of 0, 4, 17 and 18 cm lacked the planktic species, so no data for these species at those mentioned intervals (Fig.15).

3.4.1 GC3 (Gravity core)

The δ ^{13}C in the planktic species ranges between -2.33 ‰ (least value) at 132-133 cm and 0.73‰ (highest value) at 50-51cm (Fig.13a) and has an average value of -0.04 ‰ while its δ ^{18}O ranges between 1.36 ‰ (least value) at 63-64cm and 5.00 ‰ (highest value) at 115-116 cm (Fig.13a), with an average value of 3.60 ‰. The least value of δ ^{13}C is 2.29 ‰ below the average value (-0.04 ‰) while its highest value is 0.77 ‰ above the average. The least value of δ ^{18}O is 2.24 ‰ below the average value (3.60 ‰) while its highest value is 1.40 ‰ above the average.

In case of the benthic species, the δ ^{13}C values ranges between -12.73 ‰ (least value) at 132-133 cm and 1.26 ‰ (highest value) at 40-41 cm (Fig.13b), with an average value of 0.27 ‰ while its δ ^{18}O values ranges between -0.53 ‰ (least value) at 129-130 cm and 4.84 ‰ (highest value) at 132-133 cm (Fig.13b), with an average value of 3.60 ‰. The least value of δ ^{13}C is 13.00 ‰ below the average (0.27 ‰) while its highest value is 0.99 ‰ above average value. The least value of δ ^{18}O is 4.13 ‰ below the average value (3.60 ‰) while its highest value is 1.24 ‰ above average.

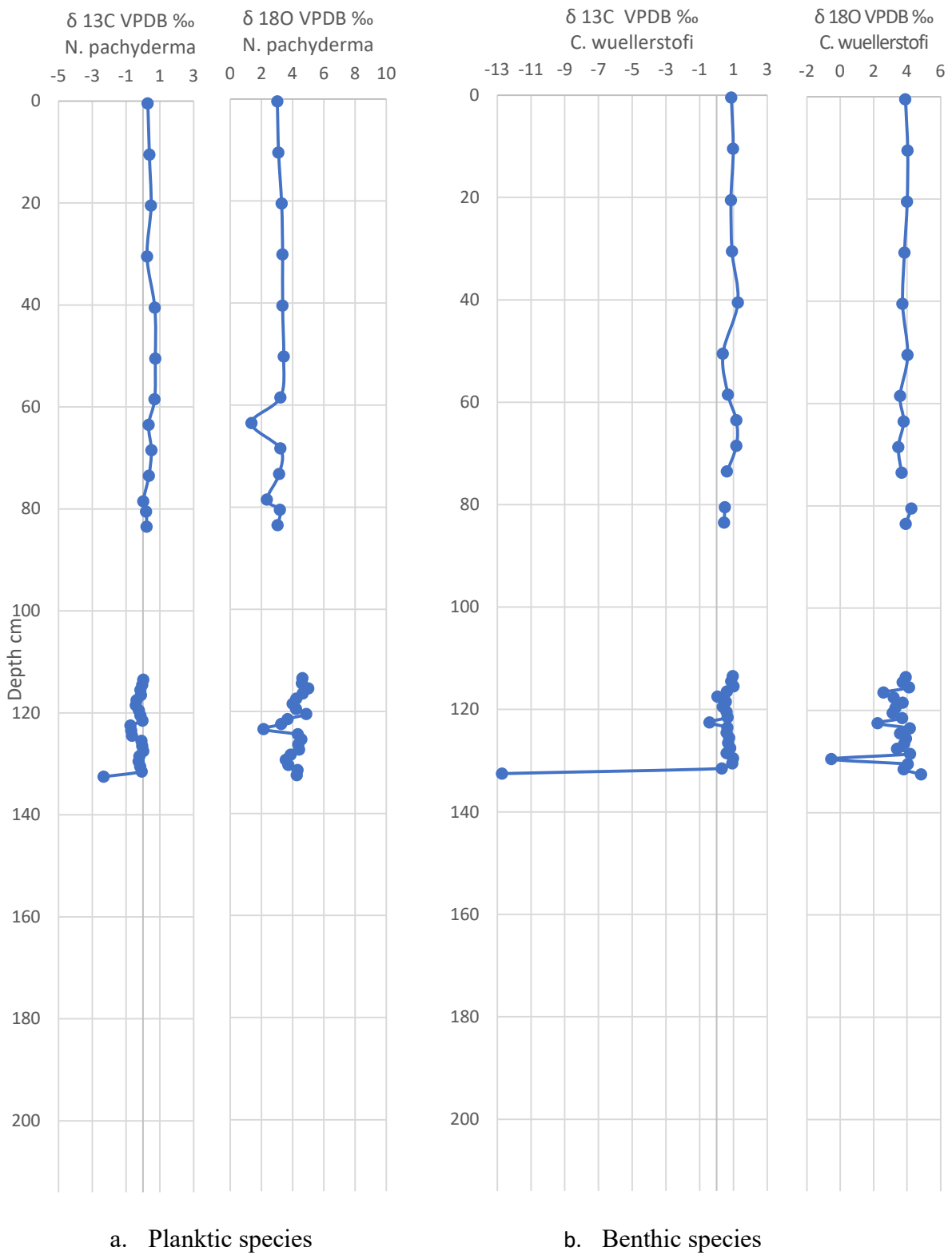

Fig.13: Stable isotopes of carbon and oxygen from the gravity core (GC3) plotted against depth (a). Planktic *Neogloboquadrina pachyderma* (b). Benthic *Cibicides wuellerstofi*

3.4.2 PusC-7 (Push core)

The planktic species have their average values of δ ^{13}C and δ ^{18}O as 0.30 ‰ and 3.00 ‰ respectively while the benthic species have the average values of δ ^{13}C and δ ^{18}O as 0.60 ‰ and 3.95 ‰ respectively. In the planktic species, the δ ^{13}C and δ ^{18}O plots with respect to depth trend in similar way in terms of alternate increase and decrease in values as depth increases (Fig.14a). There is a highest peak of 0.62 ‰ (δ13C) at 10-11 cm, which is 0.32 ‰ increase above the average value while a least peak of -0.15 ‰ at 24-25 cm, which corresponds to 0.45 ‰ decrease below the average value (0.30 ‰). The δ ^{18}O is highest at 12-13 cm and 33-34 cm with a value of 3.50 ‰ (Fig.14a), which is 0.50 ‰ increase above the average (3.00 ‰) and with the least value of 0.77 ‰ at 8-9 cm, which is 2.23 ‰ decrease below the average value.

In the benthic species, the trend is opposite for δ ^{13}C and δ ^{18}O at 6-7 cm, 38-39 cm and 40-41cm, but similar at 25-26 cm and 31-32 cm (Fig.14b). The δ ^{13}C has the least peak of -0.81 ‰ at 14-15 cm (Fig.14b), which is 1.41 ‰ decrease below average (0.60 ‰) and the highest peak of 1.17 ‰ at 36-37 cm, which is 0.57 ‰ increase above the average value. In case of δ ^{18}O, a least peak of 1.60 ‰ is observed at 6-7 cm, which is 2.35 ‰ decrease below the average (3.95 ‰) and a highest peak of 4.18 ‰ at 15-16 cm, which is 0.23 ‰ increase above the average value (Fig.14b).

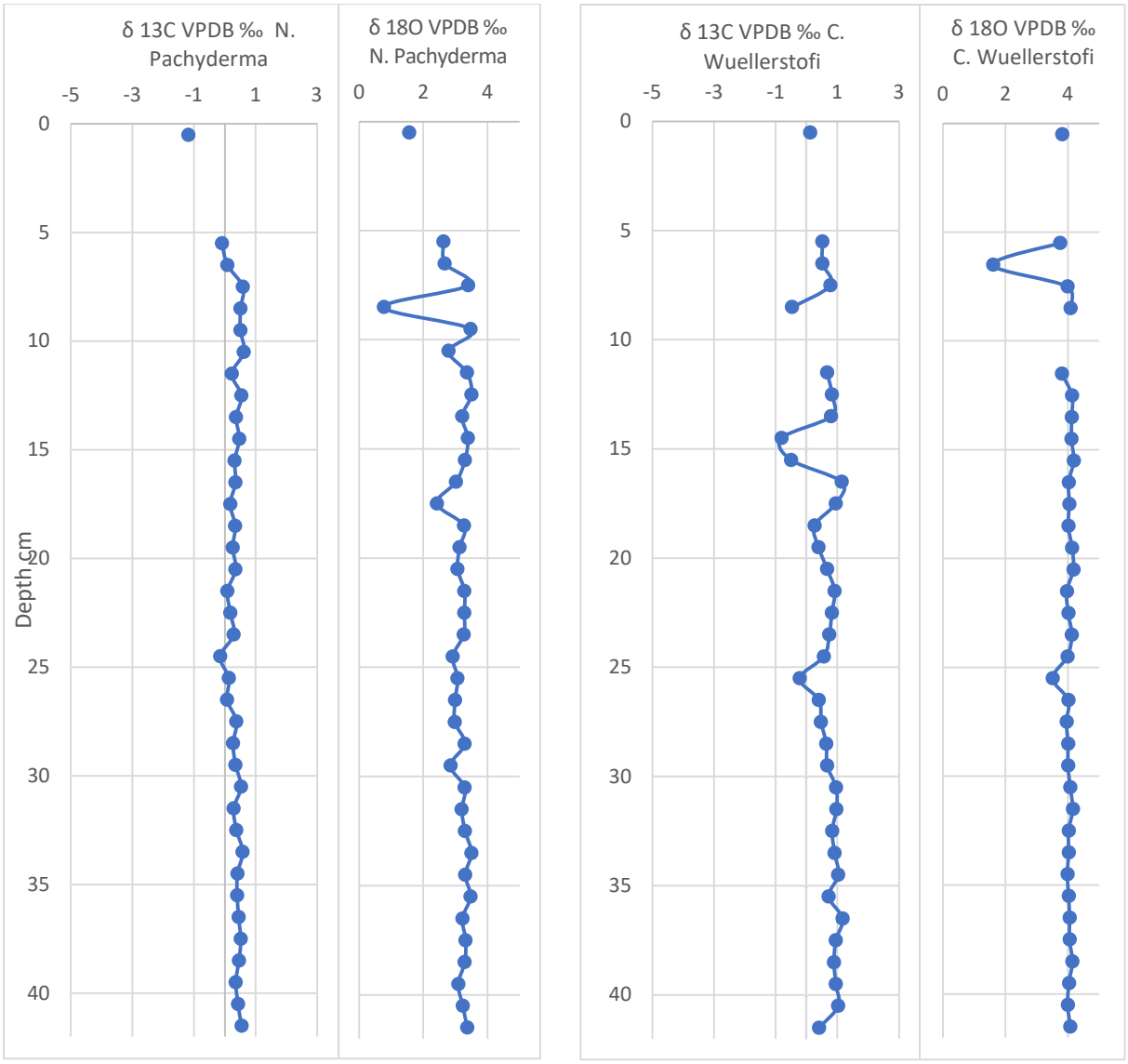

a. Planktic species b. Benthic species

Fig.14: Stable isotopes of carbon and oxygen from the Push (Reference) core (PusC7) plotted against depth (a). Planktic *Neogloboquadrina pachyderma* (b). Benthic *Cibicides wuellerstofi*

3.4.3 BlaC -3 (Blade core)

The δ ^{13}C and δ ^{18}O average values of the planktic species -0.88 ‰ and 3.08 ‰ respectively. The least values of δ ^{13}C and δ ^{18}O are -1.36 ‰ at 20cm and 2.62 ‰ at 19 cm respectively (Fig.15a). The δ ^{13}C least value is 0.48 ‰ decrease below the average value (-0.88 ‰) and the δ ^{18}O least value is 0.46 ‰ decrease below the average value (3.08 ‰). The highest values of δ ^{13}C and δ ^{18}O are -0.51 ‰ at 16 cm and 3.30 ‰ at 15 cm respectively (Fig.15a), and they are above their average values by 0.37 ‰ (δ ^{13}C) and 0.22 ‰ (δ ^{18}O).

In case of the benthic species, the δ ^{13}C and δ ^{18}O average values are -1.98 ‰ and 3.87 ‰ respectively. The least values of δ ^{13}C and δ ^{18}O are -3.94 ‰ at 20 cm and 3.48 ‰ at 4 cm respectively (Fig.15b). The least δ ^{13}C value is 1.96 ‰ decrease below the average value (-1.98 ‰), and the least δ ^{18}O value is 0.39 ‰ below the average value (3.87 ‰). The highest values of δ ^{13}C and δ ^{18}O are 0.98 ‰ at 0 cm and 4.22 ‰ at 20 cm respectively (Fig.15b), and they are above their average values by 2.96 ‰ (δ ^{13}C) and 0.35 ‰ (δ ^{18}O).

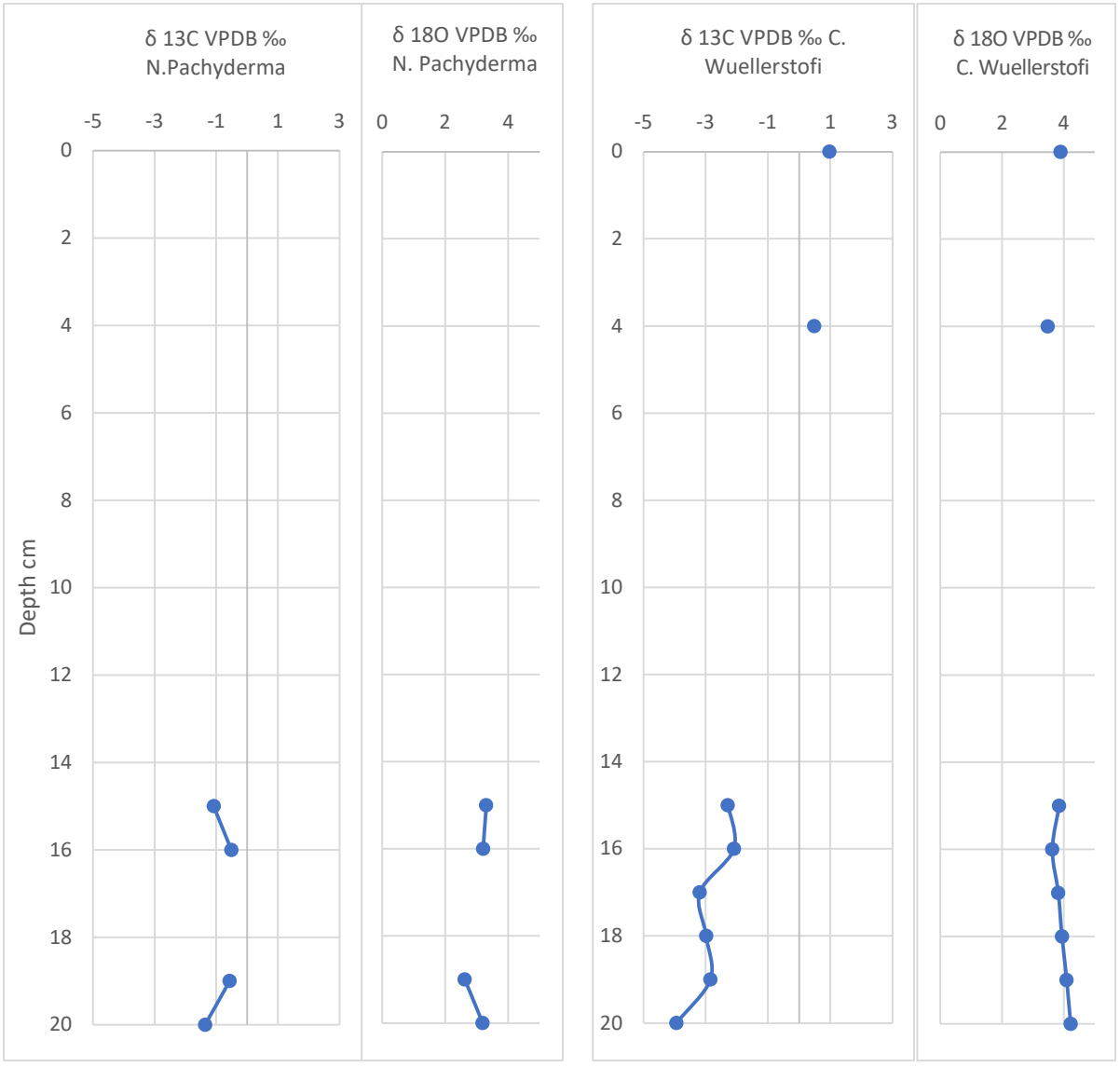

a. Planktic species b. Benthic species

Fig.15: Stable isotopes of carbon and oxygen from the Blade core (BlaC3) plotted against depth (a). Planktic *Neogloboquadrina pachyderma* (b). Benthic *Cibicides wuellerstofi*

CHAPTER 4

4. Discussion and Interpretation

4.1 Lithology and Chronology

The chronostratigraphic approach is based on the identification of the main lithostratigraphic units in relation to Late Weichselian deglaciation as in the work of Schneider et al., (2018) on Vestnesa Ridge (NW Svalbard). I aim to find evidence of sediment deposition through meltwater plumes and iceberg rafting, also affecting the sediment organic matter inventory (marine vs terrestrial inputs). The sediment of the gravity core CAGE21_1KH04_GC3 is sub-divided into two units based on sediment properties such as grain sizes (Zr/Rb ratio), fossil contents (Ca/Ti ratio and visual observation of bivalve shells) and organic geochemistry (C/N atomic ratio) coupled with the Fe/Ca ratio. The latter shows changes in signal to mark transition points which corresponds with sediment colour as shown by the XRF imagery (Fig.16). Fe/Ca ratio aids in dividing the stratigraphic units as it illustrates the terrestrial debris input (high value) against the marine biogenic debris (low value). Hereafter, a unit is defined as a volume of sediment with homogenous properties and a relative age range. Each identified unit is indicative of a particular paleoenvironment. Unit I is in the upper 99 cm of the gravity core and is the Holocene sediments started depositing about 11.7 cal ka BP (Argentino et al., 2021). It is rich in sandy-mud and brownish in colour, with C/N values between 8.9 and 14.5, mostly falling below 10 indicating a dominant marine organic component. This interpretation is also consistent with the high Ca/Ti ratio related to biogenic debris. Unit II is 99 cm to the bottom of the gravity core and consists of dark grey silty mud and fine-grained sand deposited by sea ice melt suggesting cyclic sedimentation. There is appearance of ice-rafted debris (IRDs) lodged in the gravity core, which caused a remarkable increase in Zr/Rb ratio between depths 120 and 140 cm (Fig.16). It has a shell layer with the highest Ca/Ti peak at 129 cm. It has C/N values between 22 and 29, suggesting terrestrial input of organic matter. This unit is barren in foraminifera from 134 cm to the bottom of the gravity core. The lack of foraminifera towards the bottom of the core and presence of IRDs led to the assumption that Unit II was deposited in permanent sea ice setting which resulted in settling of fine-grained sediments and slowed down biological activity (Eynaud et al., 2009; Patel, 2018). Tubeworms recrystallised in pyrites are scattered within this unit. Pyrite is formed from the reaction between Hydrogen sulfide (H_2S) from

bacterial sulfate reduction and iron oxides. This unit is a low oxygen environment as it favours pyrite formation. This unit is ascribed to the Younger Dryas-post Bølling period of about 14.5 cal ka BP.

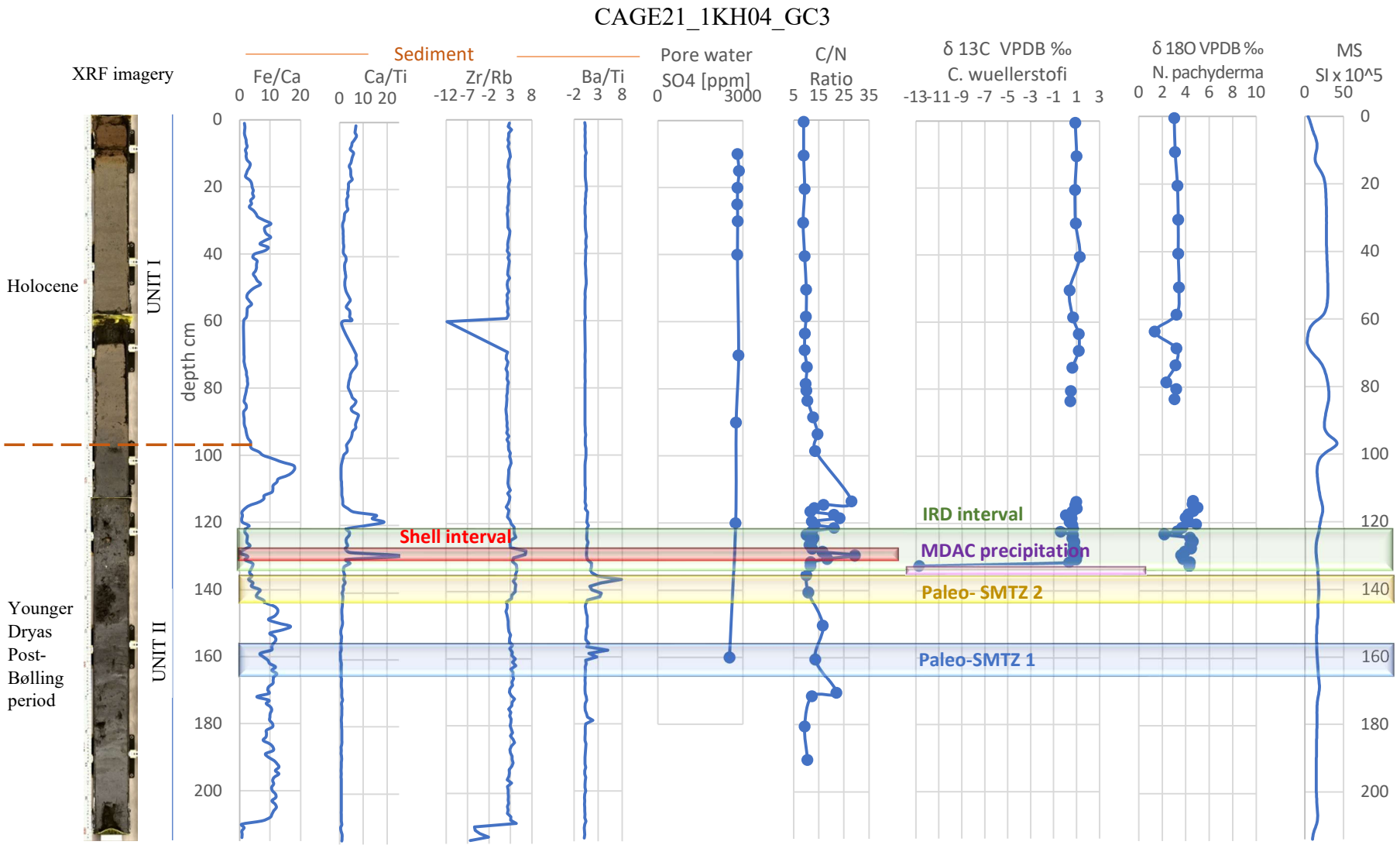

Fig.16: Chronostratigraphy, sediment and foraminiferal geochemistry, Magnetic susceptibility and porewater data of the gravity core CAGE21_1KH04_GC3.

4.2 Stable Isotope Records

4.2.1 Carbon Isotopes

The δ ^{13}C values of the planktic *N. pachyderma* sin from the Push core (reference core) range between -0.15 ‰ and 0.62 ‰ (Fig.14a) and they are here interpreted as indicative of normal marine condition unaffected by methane seepage because they fit within the range ~ -1 to ~ +1 (Panieri et al., 2017). The δ ^{13}C values of the benthic *C. wuellerstofi* of the same core range between -0.81 ‰ and 1.17 ‰ (Fig.14b), also an indication of a normal marine condition.

The δ ^{13}C values of the *N. pachyderma* sin from the Gravity core (Fig.13a) range between -2.33 ‰ and 0.73 ‰, which could still indicate a normal marine condition, while that of the *C. wuellerstofi* range between -12.73 ‰ and 1.26 ‰. The more negative values are interpreted as indicative of diagenetic alteration due to methane-derived authigenic carbonate (MDAC) precipitation on the foraminiferal tests. Similar negative values were also interpreted as diagenetically altered foraminiferal tests from a methane seep site on Vestnesa Ridge (NW Svalbard) having strongly negative δ ^{13}C values as low as -16.86 ‰ (Schneider et al., 2017).

The available data of δ ^{13}C of *N. pachyderma* sin from the Blade core (Fig.15a) shows that δ ^{13}C values range between -1.36 and -0.51 ‰ and can be indication of normal marine conditions while the δ ^{13}C values of the benthic *C. wuellerstofi* (Fig.15b) range between -3.94 and 0.98 ‰, which could likely suggest ingestion of ^{13}C-depleted methanotrophic microbes by the foraminifera while metabolically active. This is because living foraminifera can incorporate ^{13}C-depleted microbes that feed on methane to produce a slightly negative δ ^{13}C as low as -5.6 ‰ (Panieri, 2006; Rathburn et al., 2003).

4.2.2 Oxygen Isotopes

The δ ^{18}O values of the planktic *N. pachyderma* sin from the Push core (Fig.14a) range between 0.77 and 3.47 ‰; in the Gravity core, it ranges between 1.36 and 5.00 ‰ (Fig.13a) and that of the Blade core (Fig.15a) ranges between 2.62 and 3.3 ‰. The δ ^{18}O values as low as 2.8 to 3 ‰ were obtained at the Vestnessa Ridge for *N. pachyderma* sin in Post-Last Glacial Maximum (17.8-16.7 ka BP) aged sediments, and during the Last Glacial

Maximum (23.5-24 ka BP) in the Fram Strait, it ranges around 4.5 to 4.8 ‰ (Schneider et al., 2018; Elverhøi et al., 1995). Some of the δ ^{18}O values of the *N. pachyderma* sin in this study are similar to those of the Vestnessa Ridge while some are similar to those of the Fram Strait, indicating an age range of Last Glacial Maximum to Post-Last Glacial Maximum. Also, low δ ^{18}O values could be indication of melt-water contributions from the Svalbard-Barents Sea Ice Sheet (SBIS) which could be seen across the whole North Atlantic (Schneider et al., 2018; Elverhøi et al., 1995).

4.3 Organic Compound Records

4.3.1 Organic Carbon Concentration (%C)

The sediments of the Push core, gravity core and blade core contain organic carbon ranging between 0.24 and 0.80 % (Fig.10); 0.10 and 1.89 % (Fig.11), 0.18 and 0.68 % (Fig.12) respectively. This implies that the sediments are low in organic matter throughout the three cores. Organic carbon concentration is an indication of productivity (Meyers, 1994), so this study area falls within a low productivity setting.

4.3.2 Carbon/Nitrogen (C/N) Atomic Ratio

The C/N ratios are used to differentiate between marine and continental plant sources of sedimentary organic matter. The C/N ratios remain between 7.99 and 10 in the Push core (Fig.10), except at depths 2-3 cm, 12-14 cm, and 18-19 cm where C/N values range between 11 and 12.5. C/N values between 7.99 and 10 indicate a predominantly marine origin for the sedimentary organic matter, as interpreted by Meyers (1994) that C/N values between 4 and 10 indicate marine algae source while values between 11 and 18 signify mix of land-derived and marine-derived organic matter source. In the gravity core, the ratios fall nicely within the range of 8.74 to 10 in the first 83 cm, and at depths 171 cm to 190 cm (Fig.11) while depths 88-98 cm and 114-130 cm have C/N values between 11 and 18. The sudden rise in C/N values to 27.9, 29.1 and 22 at depths 113 cm, 129 cm and 170 cm respectively in the gravity core (Fig11) [intervals bounded by red dotted-line rectangles] indicates intervals characterised by terrestrial organic matter input (Meyers, 1994). In the blade core, C/N values between 7.77 and 10 is maintained at depths 0-5 cm and 13-20 cm, indicating a marine source of organic matter, and C/N values between 11 and 15 at depths 6-7 cm and 9-11 cm (Fig.12), indicating mix of land-derived and marine-derived source of organic matter.

4.4 Porewater Geochemistry

4.4.1 Sulfate data of Push core (PusC7)

The porewater sulfate data from the Push (reference) core (Fig.17) shows undetectable sulfate reduction. This suggests absence of Anaerobic Oxidation of Methane (AOM) process in the sediment interval. This could be accounted for by the low organic carbon productivity (%C) within the sediments that could not bring about the reduction of the sulfate, The δ ^{13}C data (Fig.17) of both the *Neogloboquadrina pachyderma* and *Cibicides wuellerstofi* indicate normal marine conditions (unaffected by methane seepage).

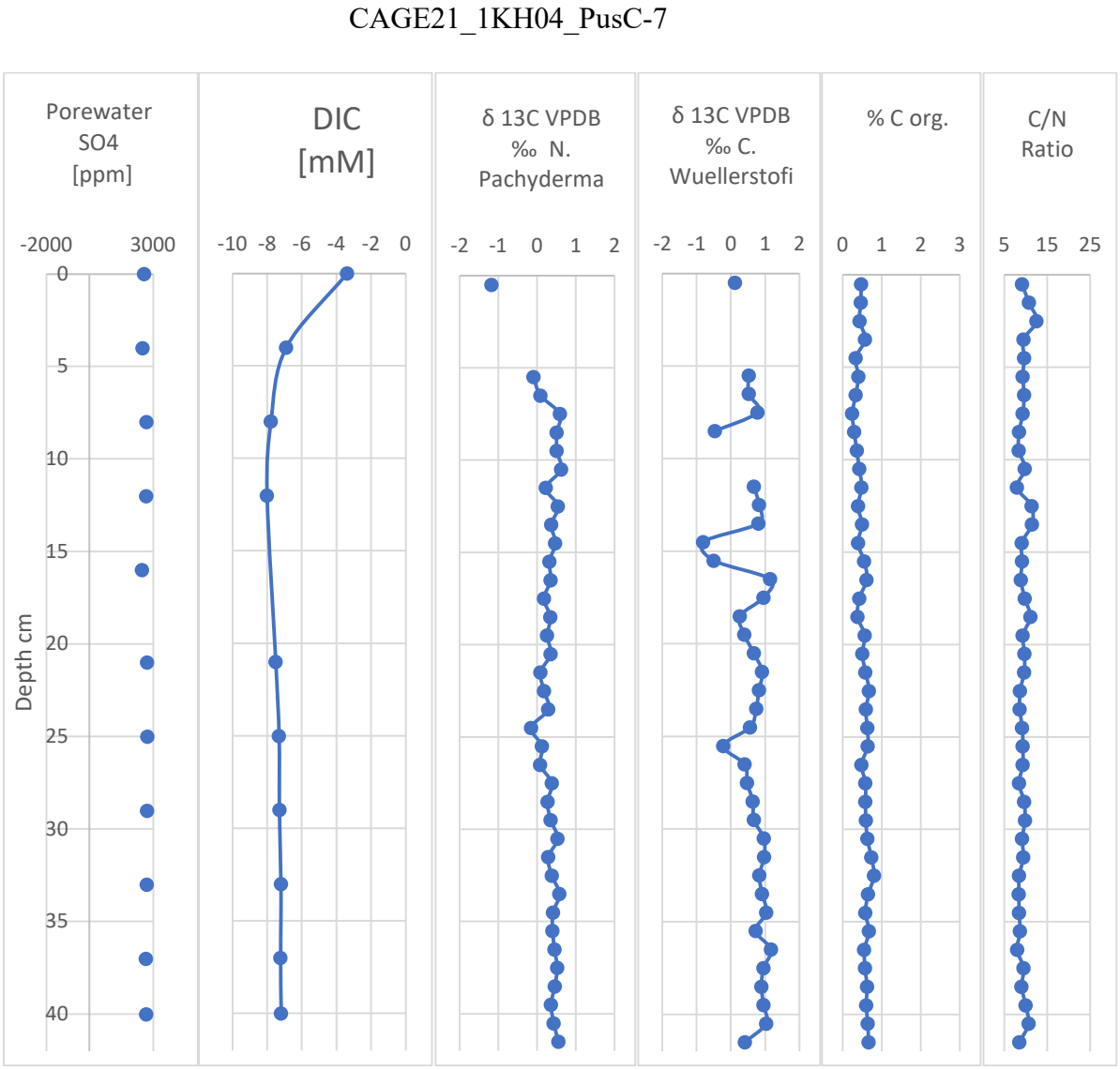

Fig.17: Integration of porewater sulfate, DIC with δ ^{13}C of the tests and sediment organic compound of the Push (PusC-7) (Reference) core.

4.4.2 Sulfate data of Blade core (BlaC3)

The porewater sulfate data from the Blade core shows a present sulfate-methane transition zone (SMTZ) at a depth of 5 cm (Fig.18), indicating that sulfate has been reduced by methane at a shallow depth. There is a methane influence at this depth towards the seafloor as seen in the sediments δ $^{13}C_{org}$ values of -29.5 to -32.1 ‰ (Fig.12) [interval bounded by green-dotted rectangle]. This implies that methane migration to this shallow depth might have taken a lot of time due to low organic matter productivity, although the available δ ^{13}C value of the benthic *C. wuellerstofi* tests around this depth (Fig.18) is 0.49 ‰ (normal marine condition). This could be that the methane influence was not so strong to have impacted the foraminiferal tests. Also, sediments of the blade core were recovered from the site inhabited by bacterial mats and tubeworms (Table 1), which are indications of slow and diffuse fluid flow (schneider et al., 2018).

CAGE21_KH04_BlaC-3

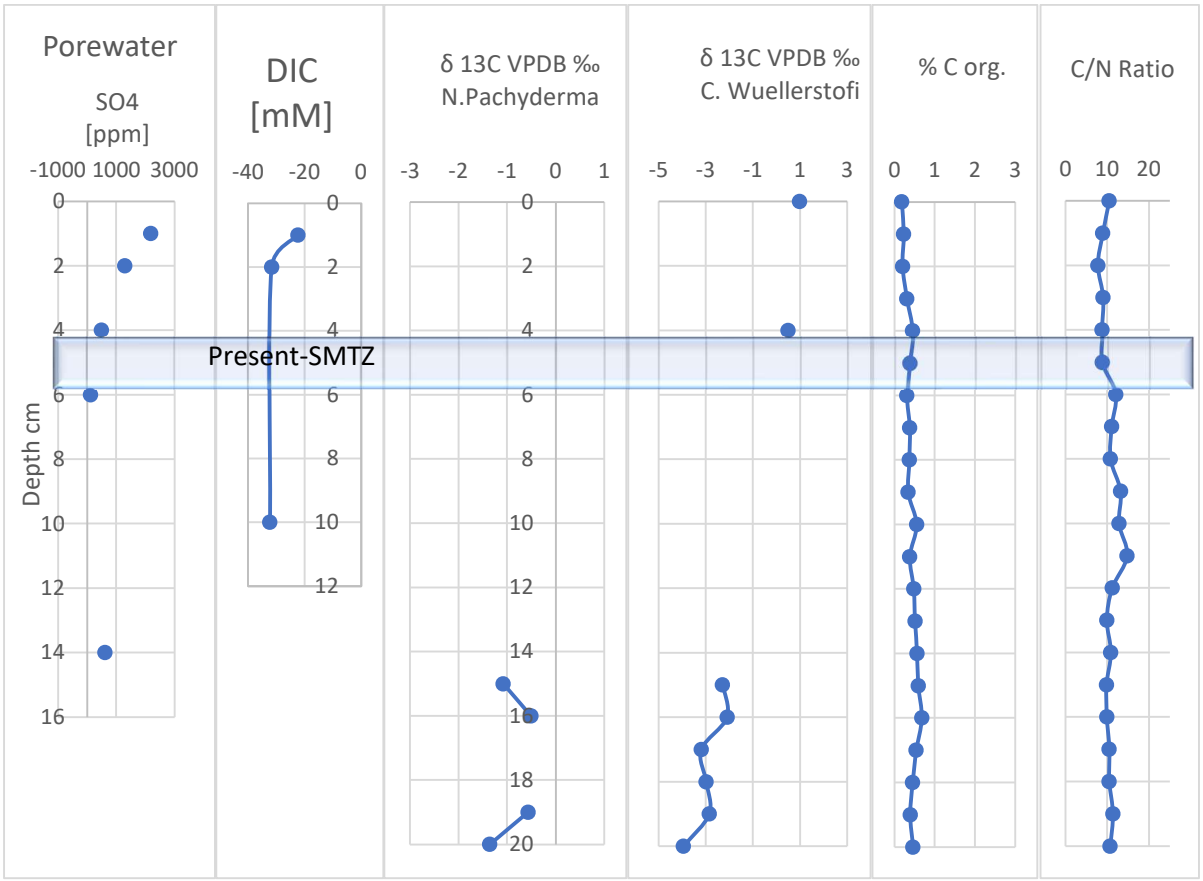

Fig.18: Integration of porewater sulfate, DIC with δ ^{13}C of the tests and sediment organic compound of the Blade core (BlaC-3).

4.4.3 Sulfate data of Gravity core (GC3)

The porewater sulfate data from the gravity core (GC3) shows undetectable present sulfate-methane transition zone (SMTZ) up to a depth of 160 cm (Fig.19). It may be that the present SMTZ position is at a deeper depth which the gravity core did not reach.

CAGE21_1KH04_GC3

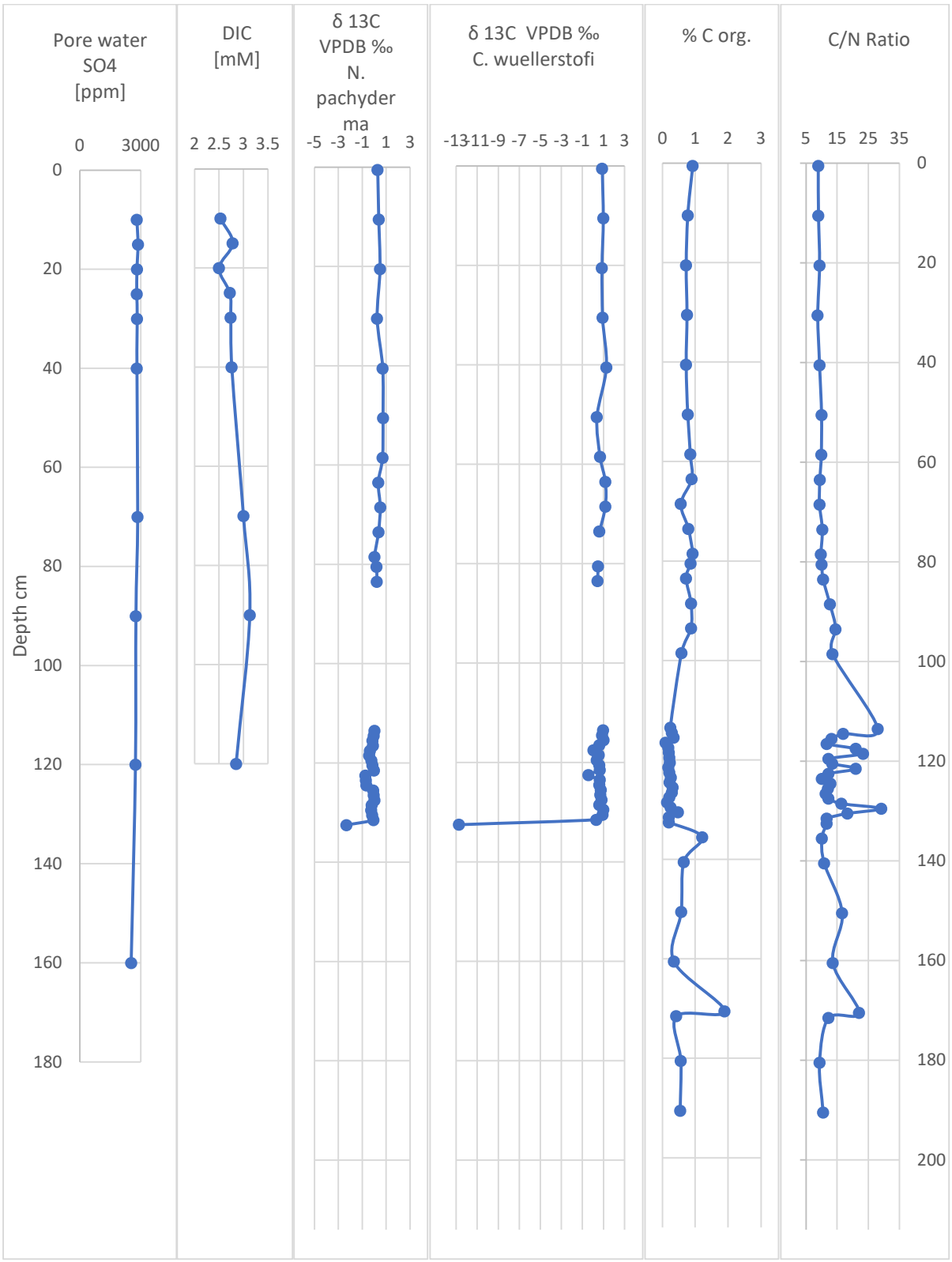

Fig.19: Integration of porewater sulfate, DIC with δ ^{13}C of the tests and sediment organic compound of the Gravity core (GC3)

4.5 X-Ray Fluorescence (XRF) Records

Elevated Ca/Ti ratios indicate sediment intervals with high calcium carbonate concentration, which could be biogenic debris like foraminiferal tests or shells or inorganic methane-derived authigenic carbonates (MDAC) precipitates (Schneider et al., 2018). Peaks in Ca/Ti at depths 127- 131 cm (Fig.16) is caused by Bivalve shells at this interval.

The Zr/Rb ratio is an indication of grain size, and it rises as the particle size of the sediment increases (Yao et al., 2020). The negative peaks at depths 60 and 212 cm (Fig.16) coincide with the empty spaces within the gravity core, so they are artifacts. The peaks between depths 121 to 138 cm are fragments of rocks (Pebbles). The pebbles dominate the shell interval. These pebbles were most likely deposited as Ice -Rafted Debris, IRD (sediments of varying grain sizes carried by floating ice and dropped into any aqueous environment) and are not representative of the site's underlying geology. The bivalve shells were found within the pebbles, IRD interval (Fig.16). This could probably be that they were product of the same event. The bivalve shells could have been transported and deposited alongside the pebbles by the floating ice. Also, the C/N ratio of the sediments at this interval is between 20.9 and 29.1, suggesting terrestrial input. This could mean that the bivalve shell fragments were transported alongside the terrestrial debris into the marine environment.

4.6 Migration of SMTZ in the gravity core sediment

The Ba/Ti ratio is an indication of the vertical shift in the position of the SMTZ, as it peaks immediately above SMTZ to form barite front (Yao et al., 2020). Barite is destabilized and dissolved as barium and sulfate ions in sulfate-depleted sediments below the SMTZ. The dissolved barium is transported over the SMTZ as the fluids move upwards, and when it encounters sulfate above the SMTZ, barite precipitates, forming a barite front (Yao et al., 2020). For the gravity core, the porewater sulfate data shows undetectable present-SMTZ up to a depth of 160 cm, which might probably be at a deeper depth which the gravity core did not reach during recovery. Two different barite fronts were identified as indications of paleo-SMTZs based on the Ba/Ti peaks at depths 158 cm and 137 cm as paleo-SMTZ 1 and paleo-SMTZ 2 respectively (Fig.16). The deeper barite front (paleo-SMTZ 1) was the first to be formed while the upper one (paleo-SMTZ 2) is the most recent. This is because old barite fronts tend to dissociate into barium and sulfate ions below the SMTZ, also it is smaller

compared to the most recent due to dissociation. Both Paleo-SMTZs correspond with the reduction in the magnetic susceptibility values at their intervals (Fig.16) due to the reduction of iron-oxides in the sediments by sulfide which is abundant at seeps because of AOM to form pyrites (Yao et al., 2020; Schneider et al., 2018). The sediments at these intervals were characterised by the presence of several pyrite tubes (Fig.20). Both paleo-SMTZs (Fig.16) are at deeper depths than the present-SMTZ of the Blade core (Fig.18), suggesting low methane flux, although their relative positions show an increase in methane flux over time. On the other hand, if the present-SMTZ were to be at a deeper depth greater than those of the identified paleo-SMTZs, it means a downward shift in the SMTZ position till present day, which is a strong indication of decrease in methane flux.

The Sulfate-Methane Transition Zones might not necessarily correspond to seafloor emissions. This is because during AOM, it is uncertain whether all the methane were consumed by methanotrophic microbes or fractions of it migrated towards the seafloor, as there were no foraminiferal tests at those depths that could record methane influence but the low negative $\delta\ ^{13}C$ value (-12.73 ‰) of the foraminiferal tests at depth 132-133 cm, few cm above the paleo-SMTZ 2 interval is an indication of MDAC precipitation(Fig.16) which is a secondary overgrowth on the primary tests, showing that methane has diffused upward to that depth and totally consumed by AOM consortia at that interval. This is because the $\delta\ ^{13}C$ of the foraminiferal tests in the upper layer sediments did not show low negative excursion that depicts methane influence. This could be interpreted as slow diffusive flow with low methane flux. The presence of pyrite tubes in the vicinity of the SMTZs is an indication of recrystallization of tubeworms into pyrites through the reducing action of sulfides, and the presence of tubeworms suggest slow and diffusive fluid flow (Schneider et al., 2018) as at the time they were living at the paleo-seafloor, associated with a deep (Paleo-) SMTZ (not reached by the gravity core).

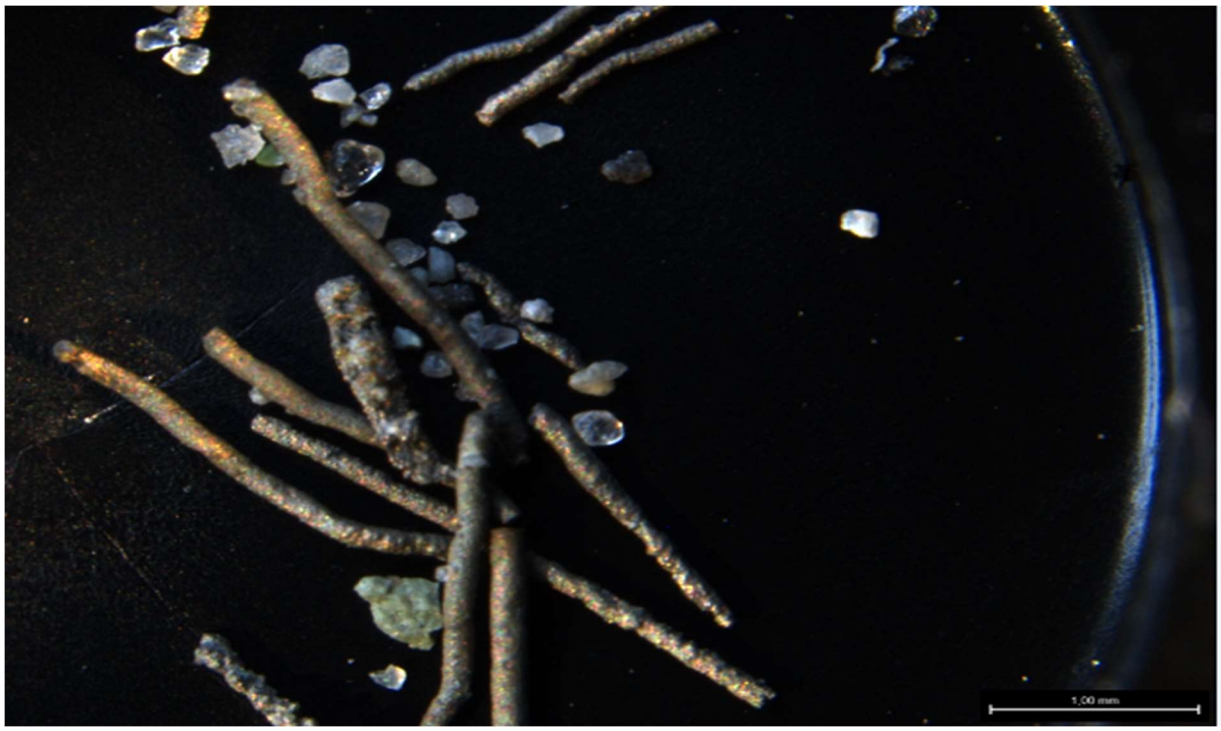

Fig.20: Pyrite tubes from the paleo-SMTZ intervals (taken from depths 140 to 160 cm sediment intervals of the gravity core, GC3).

4.7 Timing of Events

The relative time of events is based on the chronostratigraphy of the gravity core sediment (Fig.16). The paleo-SMTZs at depths 158 cm and 137 cm lie within unit II sediments, the Younger Dryas-Post Bølling period. This shows that the anaerobic oxidation of methane (AOM) processes which led to the slow and diffusive flow of methane thereby causing MDAC precipitation on foraminiferal tests at depth 132-133 cm started later than 14.5 ca ka BP (Argentino et al., 2021). The $\delta\ ^{18}O$ values decrease during the Early Holocene (Fig.16), and low $\delta\ ^{18}O$ values are indicative of melt-water contribution (Schneider et al., 2018). A slight increase in $\delta\ ^{18}O$ values in the Younger Dryas (Fig.16) is an indication of commencement of interglacial conditions which caused northward flow of warm Atlantic water masses to destabilise gas hydrates (Schneider et al., 2018; Rasmussen et al., 2007). The pebbles which were interpreted as IRDs in conjunction with the bivalve shells at depths 121 – 138 cm are also located within unit II sediments. This suggests that they were both transported from the terrestrial and deposited in the marine environment after 14.5 ka BP. Also, there were high input of terrestrial organic matter into the marine system during the last 14.5 ka BP as shown by the C/N-ratio (Fig.16) between depths 114 and 171 cm. The present-

SMTZ from the Blade core sediment is a shallow one at a depth of 5 cm, which falls within unit I sediments when compared to the gravity core sediments. This shows an on-going AOM processes in the Holocene.

4.8 Observations / Hypotheses

4.8.1 Preservation stages of the Benthic foraminifera.

Benthic *Cibicides wuellerstofi* were very well-preserved in some intervals, which suggests no diagenesis, and were not very well-preserved in some sediment intervals, leaving some fragments with partly or completely dissolved chambers. *Cibicides wuellerstofi* tests from the gravity core at 124-125 cm interval were corroded while from 127 to 133 cm were badly preserved (Fig.21). Similar cases were observed in the marine sediments from Storfjorden, Svalbard (Fig.22) as reported by Mojtahid et al. (2018). The Storfjorden, Svalbard is a zone of sea-ice formation marked by a high output of dense cascading brines (Mojtahid et al., 2018). They identified four different stages in dissolution of the tests (Fig.22):

Stage I: tests are transparent with smooth surfaces, and no sign of dissolution.
Stage II: tests have visible pores with last and or first chambers lost to dissolution.
Stage III: several chambers have been dissolved and the ones that remain have opaque wall tests.
Stage IV: tests are practically completely disintegrated, and just the organic material remains.

All these stages of dissolution were common in the Svyatogor Ridge sediment samples. The possible reason suggested by Mojtahid et al. (2018) for benthic foraminiferal tests not been well-preserved in the Storfjorden, Svalbard sediments was that the release of acidic and corrosive brines produced by the sea-ice formation could cause calcareous tests to disintegrate. This reason might possibly hold for the Svyatogor Ridge sediment intervals with this same condition because Eynaud et al. (2009) have reported corrosive bottom water and dissolution as one of the factors responsible for the Lomonosov Ridge sediments, Arctic Ocean to be entirely or partly devoid of useful calcareous microfossils.

4.8.2 Barrenness of foraminifera

Some of the sediment intervals were entirely or partly devoid of foraminiferal tests. This could be caused by sea-ice cover that slowed down biological activity (Eynaud et al., 2009). Based on prior research on the Lomonosov Ridge, Arctic Ocean, barren samples from top Pleistocene sediments represent glacial periods when there was little or no deposition or preservation of calcareous materials (Jakobsson et al., 2001; Eynaud et al., 2009). It could also be due to corrosive bottom water and dissolution (Eynaud et al., 2009). If the porewaters close to those intervals are corrosive to foraminiferal tests, they may dissolve when buried in these corrosive porewaters.

4.8.3 Low diffusive flow

Based on the positions of the paleo-SMTZs in the gravity core and the presence of tubeworms that recrystallized into pyrite tubes, methane flux could be said to be of low diffusive flow. Previous works on Svyatogor Ridge, Arctic Ocean by Johnson et al. (2015) and Waghorn et al. (2018) stated that the site hosts extensive gas hydrates. It could be the gas hydrates that serve as barricades preventing or slowing down the upward migration of fluids (Waghorn et al., 2018).

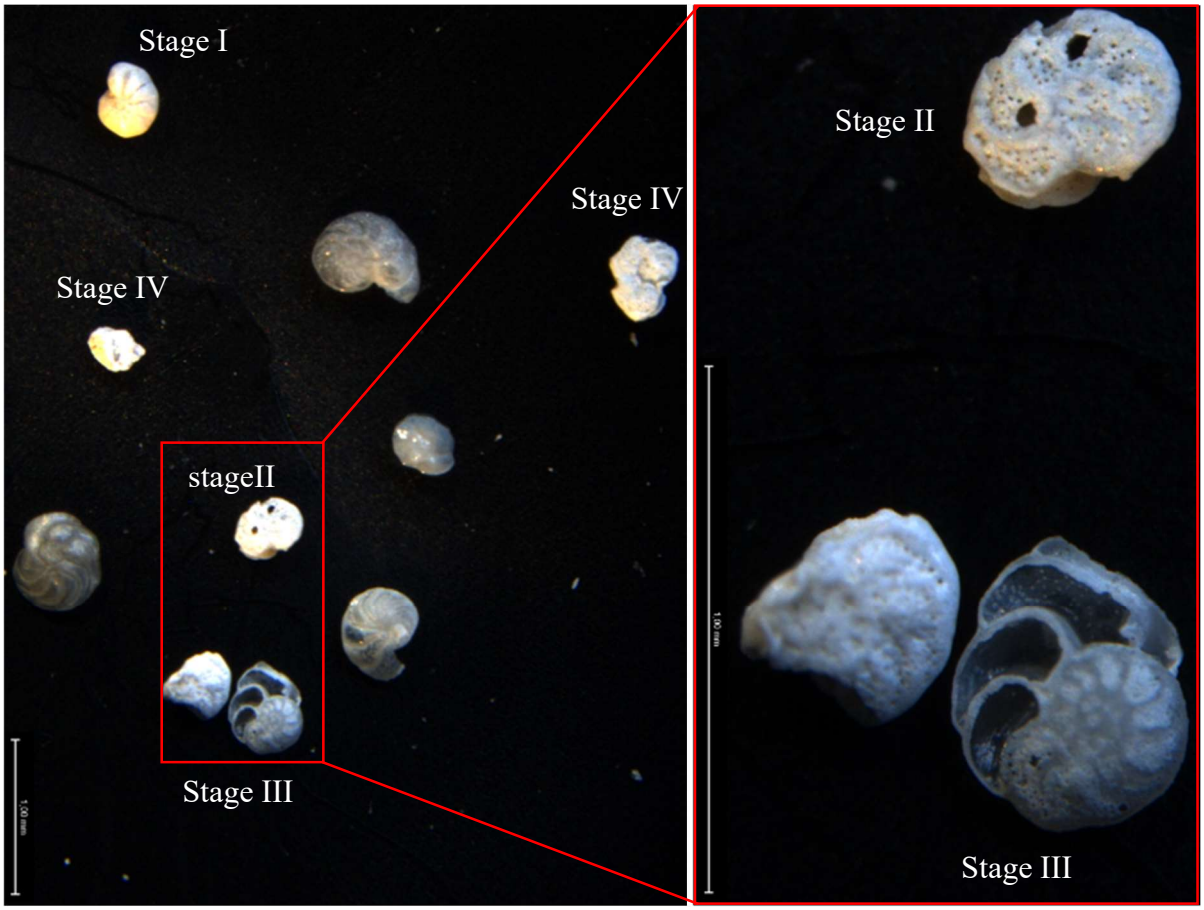

Fig.21: Stages of preservation of Benthic foraminifera in this study (taken from 127 to 133 cm sediment intervals of the gravity core, GC3).

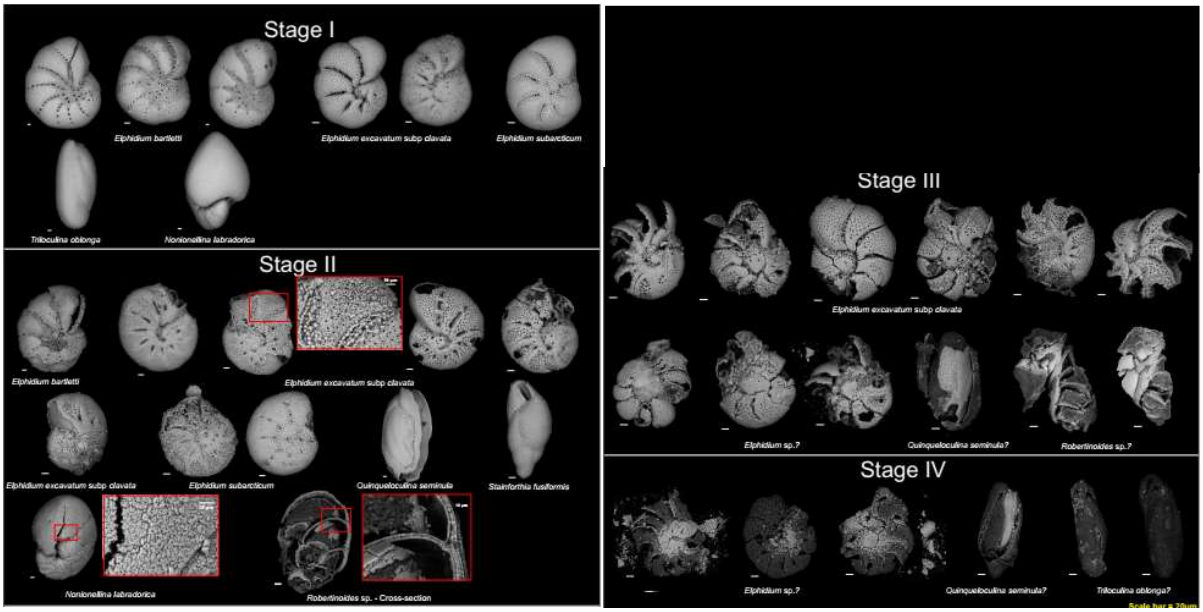

Fig.22: Stages of preservation of Benthic foraminifera from Storfjorden, Svalbard (Mojtahid et al., 2018).

CHAPTER 5

5. Summary and Conclusion

The porewater geochemistry of the reference (Push) core does not show any evidence of AOM (Fig.17). The porewater data of the blade core (Fig.18) is an indication of AOM at a shallow depth close to the seafloor, which suggests high methane flux while that of the gravity core, GC3 shows undetectable present-SMTZ (Fig.19). The sediment XRF record of the gravity core (Fig.16) shows two paleo-SMTZs at greater depths from the seafloor. Both paleo-Sulfate-Methane Transition Zones are indications of Anaerobic Oxidation of Methane processes where methane is consumed by microbes using sulfate in the porewater present in the sediment column but may not usually correspond to seafloor seepage. This is because the $\delta\ ^{13}C$ of the foraminiferal tests in the sediments did not reveal low negative excursion except for the strongly negative value at few cm above the paleo-SMTZ 2 in the gravity core that indicates methane-derived authigenic carbonate precipitation on the tests, also it is unclear if all the methane was eaten up by methanotrophic microorganisms or if fractions of it diffused to the seafloor. Based on the chronostratigraphy of the gravity core sediments, it could be inferred that the site has been an actively slow and diffusive in terms of methane seepage within the last 14.5 ka with indications of past and present AOM processes such as pyrite tubes, bacterial mats, and tubeworms, although shallow SMTZ from the Blade core sediments is an indicative of high methane flux which might be attributed to the presence of underlying small-scale faults which serve as conduits for fluid flow towards the seafloor (Waghorn et al., 2018). This could be one reason why there is variation in fluxes at this site. Other could be lateral grain size variations due to ice-rafted debris which affects fluid flow patterns. Sediments transported and deposited by ice are heterogenous (of varying grain sizes), and hence, they are poorly sorted with low permeability whereas homogenous sediments are well-sorted with high permeability (Selley, 2014).

This study shows that foraminiferal geochemistry needs the support of other proxies to give better information about paleo-seepage reconstruction. For instance, Porewater and sediment geochemistry were integrated with the stable isotopes of the foraminiferal tests to enhance the investigation of seepage at this site.

The importance of this study is that the Arctic region is one of many natural sources of methane, a greenhouse gas. Global warming is hastening the release of methane. This is because enormous amounts of methane are stored in the Arctic in natural gas deposits, permafrost, and as gas hydrates, which degrade with warming (Selley, 2014), and hence substantial methane releases from these sources may occur as a result of global warming. This has a negative impact because methane is a potent greenhouse gas. Seepage in the Arctic, and gas hydrate dissociation, can be efficiently monitored using biogeochemical proxies applied in this project, enabling geoscientists to trace the evolution of these systems under global warming.

References

Anthony, K. W., Anthony, P., Grosse, G., Chanton, J. 2012: Geologic Methane Seeps along Boundaries of Arctic Permafrost Thaw and Melting Glaciers. *Nature Science.* 5 (6), 419-426

Argentino, C., Waghorn, K. A., Vadakkepuliyambatta, S., Polteau, S., Bunz, S., Panieri, G. 2021: Dynamic and History of Methane Seepage in the Southwestern Barents Sea: New Insights from Leirdjupet Fault Complex. *Scientific Reports. Rep.* 11. 4373

Armstrong, H. A. & Brasier, M. D. 2005: Microfossils (2nd Edition). *Blackwell Publishing*

Boetius, A., Ravenschlag, K., Schubert, C. *et al.* A marine microbial consortium apparently mediating anaerobic oxidation of methane. *Nature* 407**,** 623–626 (2000). https://doi.org/10.1038/35036572

Columbia University. (no date) Stable Isotopes. Available at: http://www.columbia.edu/~vjd1/stable_isotopes.htm (Accessed: 3 March 2022).

Consolaro, C., Rasmussen, T. L., Panieri, G., Mienert, J., Bunz, S., Sztybor, K. 2015: Carbon Isotope ($\delta^{13}C$) Excursions Suggest Times of Major Methane Release During the Last 14kyr in Fram Strait, the Deep-Water Gateway to the Arctic. Climate of the Past. Vol. 11, pp. 669-685

Dessandier, P. A., Borrelli, C., Kalenitchenko, D, & Panieri, G. 2019: Benthic Foraminifera in Arctic Methane Hydrate Bearing Sediments. *Frontiers in Marine Science*. https://doi.org/10.3389/fmars.2019.00765.

Dessandier, P. A., Borrelli, C., Yao, H. *et al.* Foraminiferal $\delta^{18}O$ reveals gas hydrate dissociation in Arctic and North Atlantic ocean sediments. *Geo-Mar Lett* 40, 507–523 (2020). https://doi.org/10.1007/s00367-019-00635-6

Dessandier, P. A., Knies, J., Plaza-Faverola, A., Labrousse, C., Renoult, M., Panieri, G. 2021: Ice-Sheet Melt Drove Methane Emissions in the Arctic During the Last Two Interglacials. Geology. Vol. 49, p. https://doi.org/10.1130/G48580.1.

Elverhøi, A., Andersen, E.S., Dokken, T., Hebbeln, D., Spielhagen, R., Svendsen, J.I., Sørflaten, M., Rørnes, A., Hald, M., Forsberg, C.F., 1995. The growth and decay of the Late Weichselian ice sheet in western Svalbard and adjacent areas based on provenance studies of marine sediments. *Quat. Res.* (Duluth) 44, 303-316.

Etiope, E. & Schwietzke, S. 2019: Global Geological Methane Emission: An update of top-down and bottom-up estimates. *Elemental Science of the Anthropocene.* Vol. 7. 49

Eynaud, F., Cronin, T. M., Smith, S. A., Zaragosi, S., Mavel, J., Mary, Y., Mas, V., Pujol, C. 2009: Morphological variability of the planktonic foraminifer Neogloboquadrina pachyderma from ACEX cores: Implications for Late Pleistocene circulation in the Arctic Ocean. *Micropaleontology* 55(2)

Hill, T. M., Kennett, J. P., Spero, H. J. 2003: Foraminifera as Indicators of Methane-rich Environments: A Study of Modern Methane Seeps in Santa Barbara Channel, California. *Marine Micropaleontology*. Vol. 49, Issues 1-2, pp. 123-138. https://doi.org/10.1016/S0377-8398(03)00032-X

Jakobsson, M., Løvlie, R., Arnold, E. M., Backman, J., Polyak, L., Knutsen, J. O. and Musatov, E., 2001. Pleistocene Stratigraphy and Paleoenvironmental ariation from Lomonosov Ridge sediments, Central Arctic Ocean. *Global and Planetary Change*, 31: 1-21

Johnson, J. E., Mienert, J., Plaza-Faverola, A., Vadakkepuliyambatta, S., Knies, J., Bunz, S., Andreassen, K., Ferre, B. 2015: Abiotic Methane from Ultraslow-Spreading Ridges can Charge Arctic Gas Hydrates. *Geology*. Vol. 43, no. 5, pp. 371-374

Levin, L. 2007: Gas Promotes Mass: Methane Seeps. *American Federation of Teachers.* *https://www.aft.org>periodical>winter-2007-2008>gas*

Meyers, P. A. 1994: Preservation of Elemental and Isotopic source identification of Sedimentary organic matter. *Chemical Geology*. Vol. 114, pp. 289-302

Milkov, A.V. and Etiope, G., 2018. Revised genetic diagrams for natural gases based on a global dataset of> 20,000 samples. *Organic Geochemistry*, *125*, pp.109-120.

Millo, C., M. Sarnthein, H. Erlenkeuser, and T. Frederichs (2005a), Methane-driven late Pleistocene δ ^{13}C minima and overflow reversals in the southwestern Greenland Sea, Geology, 33, 873–876.

Millo, C., M. Sarnthein, H. Erlenkeuser, P. M. Grootes, and N. Andersen (2005b), Methane-induced early diagenesis of foraminiferal tests inthe southwestern Greenland Sea, Mar. Micropaleontol., 58, 1–12.

Miyajima, Y., Watanabe, Y., Goto, A. S., Tenkins, R. G., Sakai, S., Matsumoto, R., Hasegawa, T. 2020: Archaeal Lipid Biomarker as a Tool to Constrain the Origin of Methane at Ancient Methane Seeps: Insight into Subsurface Fluid Flow in the Geological Past. *Journal of Asian Earth Sciences.* Vol. 189

Mujtahid, M., Jouini, A., Howa, H., Lansard, B., Michel, E., Peron, O., Baltzer, A., Nardelli, M. P. 2018: Benthic Foraminiferal dissolution index for marine sediments in Storfjorden, Svalbard. *Arctic Frontiers*

Morales, C., Rogov, M., Wierzbowski, H., Ershova, V., Suan, G., Adatte, T., Føllmi, K. B., Tegelaar, E., Reichart, G., Lange, G. J., Middelburg, J. J., Schootbrugge, B. V. 2017: Glendonites Tracks Methane Seepage in Mesozoic Polar Seas. *The Geological Society of America.*

National Centers for Environmental Information (NCEI) formerly known as National Climatic Data Center (NCDC). Available at: https://www.ncdc.noaa.gov/news/what-are-proxy-data (Accessed: 14 March 2022).

Oppo, D., Siena, L. & Kemp, D. B. 2020: A Record of Seafloor Methane Seepage across the Last 150 million Years. *Scientific Reports,* 10, 2562 *https://doi.org/10.1038/s41598-020-59431-3*

Panieri, G. 2006: Foraminiferal Response to Active Methane Seep Environment: A Case Study from the Adriatic Sea. *Marine Micropaleontology*. Vol. 61, Issues 1-3, pp. 116-130. https://doi.org/10.1016/j.marmicro.2006.05.008

Panieri, G., Graves, C. A, & James, R. H. 2016: Paleo-Methane Emissions Recorded in Foraminifera Near the Landward Limit of the Gas Hydrate Stability Zone Offshore Western Svalbard. *Geochemistry, Geophysics, Geosystems*, 17, doi: 10.1002/2015GC006153

Panieri, G., Lepland, A., Whitehouse, M. J., Wirth, R., Raanes, M. P., James, R. H., Graves, C. A., Cremiere, A., Schneider, A. 2016: Diagenetic Mg-Calcite Overgrowth on Foraminiferal Tests in the Vicinity of Methane Seeps. *Earth and Planetary Science Letters*.

Panieri, G., A. Camerlenghi, I. Cacho, C. S. Cervera, M. Canals, S. Lafuerza, and G. Herrera (2012), Tracing seafloor methane emissions with benthic foraminifera: Results from the Ana submarine landslide (Eivissa Channel, Western Mediterranean Sea), Mar. Geol., 291–294, 97–112.

Panieri, G., R. H. James, A. Camerlenghi, G. K. Westbrook, C. Consolaro, I. Cacho, V. Cesari, and C. Sanchez Cervera (2014): Record of methane emissions from the West Svalbard continental margin during the last 23,500 years revealed by d13C of benthic foraminifera, Global Planet. Change, 122, 151–160.

Panieri, G. *et al.* Diagenetic Mg-calcite overgrowths on foraminiferal tests in the vicinity of methane seeps. *Earth Planet. Sci. Lett.* 458, 203–212 (2017).

Patel, J. 2018: Paleoenvironmental investigation of the northern flank of the Olga Basin (Barents Sea) during the Late Weichselian deglaciation. M.Sc Thesis. *UiT Munin Open Archive.*

Rasmussen, T.L., Thomsen, E., Slubowska, M.A., Jessen, S., Solheim, A., Koc, N., 2007: Paleoceanographic Evolution of the SW Svalbard margin (76^0N) since 20,000 C yr BP. *Quat. Res*. (Duluth) 67, 100-114.

Rathburn, A. E., Perez, M. E., Martin, J. B., Day, S. A., Mahn, C., Gieskes, J., Ziebis, W., Williams, D., Bahls, A. 2003: Relationships Between the Distribution and Stable Isotopic Composition of Living Benthic Foraminifera and Cold Methane Seep Biogeochemistry in Monterey Bay, California. *Geochemistry, Geophysics, Geosystems*. Vol. 4, Issues12. https://doi.org/10.1029/2003GC000595

Rathburn, A. E., Levin, L. A., Held, Z., Lohmann, K. C. 2000: Benthic Foraminiferal Associated with Cold Methane Seeps on the Northern California Margin: Ecology and Stable Isotopic Composition. *Marine Micropaleontology*. Vol. 38, Issues 3-4, pp. 247-266. https://doi.org/10.1016/S0377-8398(00)00005-0.

Schneider, A., Panieri, G., Lepland, A., Consolaro, C., Cremiere, A., Forwick, M., Johnson, J. E., Plaza-Faverola, A., Sauer, S., Knies, J. 2018: Methane Seepage at Vestnesa Ridge (NW Svalbard) Since the Last Glacial Maximum. *Quaternary Science Reviews*. Vol. 193, pp. 98-117. https://doi.org/10.1016/j.quascirev.2018.06.006

Schneider, A., Cremiere, A., Panieri, G., Lepland, A., Knies, J. 2017: Diagenetic Alteration of Benthic Foraminifera from a Methane Seep site on Vestnesa Ridge (NW Svalbard). *Deep-Sea Research I* .Vol. 123, pp. 22-34. http://dx.doi.org/10.1016/j.dsr.2017.03.001

Selley, R. C. 2014: Elements of Petroleum Geology (2^{nd} edition). *Academic Press.*

Waghorn, K. A., Bunz, S., Plaza-Faverola, A., Johnson, J. E. 2018: 3-D Seismic Investigation of a Gas Hydrate and Fluid Flow System on an Active Mid-Ocean Ridge; Svyatogor Ridge, Fram Strait. *Geochemistry, Geophysics, Geosystems*. Vol. 19, Issues 8, pp. 2325-2341. doi: 10.1029/2018GC007482

Waghorn, K. A., Vadakkepuliyambatta, S., Plaza-Faverola, A., Johnson, J. E., Bunz, S., Waage, M. 2020: Crustal Process Sustain Arctic Abiotic Gas Hydrate and Fluid Flow Systems. *Scientific Reports*. 10, 10679. https://doi.org/10.1038/s41598-020-67426-3

Weber, T., Wiseman, N.A. and Kock, A., 2019. Global ocean methane emissions dominated by shallow coastal waters. *Nature communications*, *10*(1), pp.1-10.

Yao, H., Niemann, H., Panieri, G. 2020: Multi-Proxy Approach to Unravel Methane Emission History of an Arctic Cold Seep. *Quaternary Science Reviews*. Vol. 244

Yao, H. 2021: Reconstruction of Past and Present Methane Emission in the Arctic Cold Seeps using Biogeochemical Proxies. *UiT Open Research Archive.*

Ziegler, M., Jilbert, T., de Lange, G. J., Lourens, L. J., Reichart, G. 2008: Bromine counts from XRF scanning as an estimate of the marine organic carbon content of sediment cores. *Geochemistry, Geophysics, Geosystems.* Vol. 9 no. 5. doi:10.1029/2007GC001932